



**Calhoun: The NPS Institutional Archive**  
**DSpace Repository**

---

Theses and Dissertations

1. Thesis and Dissertation Collection, all items

---

1976-06

# Development of a temperature-pneumatic probe and application at the rotor exit in a transonic compressor

Dodge, Fredrick James

Monterey, California. Naval Postgraduate School

---

<http://hdl.handle.net/10945/17738>

---

This publication is a work of the U.S. Government as defined in Title 17, United States Code, Section 101. Copyright protection is not available for this work in the United States.

*Downloaded from NPS Archive: Calhoun*



<http://www.nps.edu/library>

Calhoun is the Naval Postgraduate School's public access digital repository for research materials and institutional publications created by the NPS community. Calhoun is named for Professor of Mathematics Guy K. Calhoun, NPS's first appointed -- and published -- scholarly author.

**Dudley Knox Library / Naval Postgraduate School**  
**411 Dyer Road / 1 University Circle**  
**Monterey, California USA 93943**

DEVELOPMENT OF A TEMPERATURE-PNEUMATIC  
PROBE AND APPLICATION AT THE ROTOR EXIT  
IN A TRANSONIC COMPRESSOR

Fredrick James Dodge

AUDLEY KNOX LIBRARY  
4000 WALNUT STREET  
SEATTLE, WASHINGTON 98104

# NAVAL POSTGRADUATE SCHOOL

Monterey, California



## THESIS

DEVELOPMENT OF A TEMPERATURE-PNEUMATIC  
PROBE AND APPLICATION AT THE ROTOR EXIT  
IN A TRANSONIC COMPRESSOR

by

Frederick James Dodge

June 1976

Thesis Advisor:

R.P. Shreeve

Approved for public release; distribution unlimited.

T174035



UNCLASSIFIED

SECURITY CLASSIFICATION OF THIS PAGE (When Data Entered)

## REPORT DOCUMENTATION PAGE

READ INSTRUCTIONS  
BEFORE COMPLETING FORM

1. REPORT NUMBER	2. GOVT ACCESSION NO.	3. RECIPIENT'S CATALOG NUMBER
4. TITLE (and Subtitle) Development of a Temperature-Pneumatic Probe and Application at the Rotor Exit in a Transonic Compressor		5. TYPE OF REPORT & PERIOD COVERED Master's Thesis; June 1976
7. AUTHOR(s) Frederick James Dodge		5. PERFORMING ORG. REPORT NUMBER
9. PERFORMING ORGANIZATION NAME AND ADDRESS Naval Postgraduate School Monterey, California 93940		5. CONTRACT OR GRANT NUMBER(s)
11. CONTROLLING OFFICE NAME AND ADDRESS Naval Postgraduate School Monterey, California 93940		10. PROGRAM ELEMENT, PROJECT, TASK AREA & WORK UNIT NUMBERS
14. MONITORING AGENCY NAME & ADDRESS (if different from Controlling Office)		12. REPORT DATE June 1976
		13. NUMBER OF PAGES 117
		15. SECURITY CLASS. (of this report) Unclassified
		15a. DECLASSIFICATION/DOWNGRADING SCHEDULE
16. DISTRIBUTION STATEMENT (of this Report) Approved for public release; distribution unlimited.		
17. DISTRIBUTION STATEMENT (of the abstract entered in Block 20, if different from Report)		
18. SUPPLEMENTARY NOTES		
19. KEY WORDS (Continue on reverse side if necessary and identify by block number) temperature-pneumatic probe transonic compressor		
20. ABSTRACT (Continue on reverse side if necessary and identify by block number) The development is reported of a new combination temperature-pneumatic probe specifically to determine the blade element performance of the rotor in a transonic compressor. The design incorporates a fine wire thermo- couple sensor which provides a measure of temperature rise that is insensitive to Mach number. With simultaneous measurements from four pneumatic sensors, the velocity		

UNCLASSIFIED



## (20. ABSTRACT Continued)

vector was determined locally in radial surveys downstream of the compressor rotor. The probe was calibrated in a free jet. The calibration measurements were reduced to a set of equations to allow off-line reduction of compressor measurements using a Hewlett-Packard Model 9830A calculator and peripherals. The design, development, calibration, and application of the probe are described and initial results of measurements in the compressor are given.



Development of a Temperature-Pneumatic  
Probe and Application at the Rotor Exit  
in a Transonic Compressor

by

Frederick James Dodge  
Lieutenant, United States Navy  
B.S., University of Oregon, 1969

Submitted in partial fulfillment of the  
requirements for the degree of

MASTER OF SCIENCE IN AERONAUTICAL ENGINEERING

from the  
NAVAL POSTGRADUATE SCHOOL  
June 1976

thesis  
D617  
c.1

ABSTRACT

The development is reported of a new combination temperature-pneumatic probe specifically to determine the blade element performance of the rotor in a transonic compressor. The design incorporates a fine wire thermocouple sensor which provides a measure of temperature rise that is insensitive to Mach number. With simultaneous measurements from four pneumatic sensors, the velocity vector was determined locally in radial surveys downstream of the compressor rotor. The probe was calibrated in a free jet. The calibration measurements were reduced to a set of equations to allow off-line reduction of compressor measurements using a Hewlett-Packard Model 9830A calculator and peripherals. The design, development, calibration, and application of the probe are described and initial results of measurements in the compressor are given.



## TABLE OF CONTENTS

I.	INTRODUCTION -----	12
II.	THE TRANSONIC COMPRESSOR -----	15
	A. DESCRIPTION -----	15
	B. INSTRUMENTATION -----	16
	C. ROTOR PERFORMANCE DETERMINATION USING A COMBINATION PROBE -----	17
III.	PROBE DESIGN -----	19
	A. DESCRIPTION -----	19
	B. PNEUMATIC SENSOR DESIGN -----	19
	C. THERMOCOUPLE SENSOR DESIGN -----	22
	1. Background -----	22
	2. Initial Design and Test Results -----	24
	3. Final Design and Test Results -----	25
IV.	PROBE CALIBRATION TEST RESULTS -----	28
	A. METHOD OF APPROACH -----	28
	B. THE PNEUMATIC CALIBRATION -----	29
	C. THE THERMOCOUPLE CALIBRATION -----	36
V.	APPLICATION IN THE TRANSONIC COMPRESSOR -----	40
VI.	CONCLUSIONS -----	44
	FIGURES -----	47
	APPENDIX A: FABRICATION OF THE THERMOCOUPLE SENSOR ---	86
	A.1 INTRODUCTION -----	86
	A.2 EQUIPMENT AND MATERIALS -----	87
	A.2.1 Equipment -----	87
	A.2.2 Materials -----	88



A.3	FABRICATION OF THE INSULATOR NOTCH -----	89
A.4	FABRICATION OF THE SENSOR -----	90
A.4.1	Spot Welding -----	94
FIGURES	-----	95
APPENDIX B:	IMPROVEMENTS TO THE PROBE CALIBRATION	
	APPARATUS -----	103
B.1	INTRODUCTION -----	103
B.2	PROBE MOUNTING BOX -----	104
B.3	PITCH ANGLE SURVEY MOUNT -----	105
B.4	HONEYCOMB SECTION FOR THE SWIRL ANNULUS -----	106
FIGURES	-----	107
APPENDIX C:	COMPUTER PROGRAMS -----	111
BIBLIOGRAPHY	-----	116
INITIAL DISTRIBUTION LIST	-----	117



# LIST OF ILLUSTRATIONS

	PAGE
1. Schematic of the Compressor Test Rig -----	47
2. Compressor Assembly -----	48
3. Drawing of the Combination Probe -----	49
4. Photographs of the Combination Probe -----	50
5. The Pneumatic Sensor Tip -----	51
6. Pitch Angle Sensitivity to a 32 mil Tube ----	52
7. Yaw Angle Sensitivity to a 32 mil Tube -----	53
8. Combination Probe Test Apparatus -----	54
9. (P1-P4) vs. Pitch Angle for Nine Velocities -	55
10. (P1-P23) vs. Pitch Angle for Nine Velocities -----	56
11. Pitch Angle vs. Beta (Initial Survey) -----	57
12. Schematic of Initial Thermocouple Sensor Design -----	58
13. Initial Geometry for Thermocouple Housing Tube -----	59
14. Temperature Variation with Phi and Mach Number for Initial Thermocouple Design -----	60
15. Schematic of Final Thermocouple Sensor Design -----	61
16. Photographs of Insulator Notch -----	62
17. Temperature Variation with Phi and Mach Number for Final Thermocouple Design -----	63
18. Beta vs. Phi from Calibration Data -----	64
19. Gamma vs. Phi from Calibration Data -----	65
20. X vs. Beta from Calibration Data -----	66



	PAGE
21. $A_1$ Coefficients vs. X from Calibration Data ---	67
22. B0 Coefficients vs. Phi from Calibration Data -----	68
23. B1 Coefficients vs. Phi from Calibration Data -----	69
24. B2 Coefficients vs. Phi from Calibration Data -----	70
25. B3 Coefficients vs. Phi from Calibration Data -----	71
26. B4 Coefficients vs. Phi from Calibration Data -----	72
27. B5 Coefficients vs. Phi from Calibration Data -----	73
28. X vs. Beta from Polynomial Expressions -----	74
29. Velocity Profiles for a Traverse of the 4.2 Inch Nozzle -----	75
30. Recovery Factor vs. Mach Number for the Thermocouple Calibration -----	76
31. Thermocouple Calibration Curve and Coefficients -----	77
32. Temperature Calibration Coefficients -----	78
33. Results of Probe Surveys Downstream of the Transonic Compressor (50% Design Speed) -----	79
34. Results of Comb. Probe and NASA Probe Surveys Downstream of the Transonic Compressor Rotor (50% Design Speed) -----	80
35. Results of Probe Surveys Downstream of the Transonic Compressor (65% Design Speed) -----	81
36. Results of Comb. Probe and NASA Probe Surveys Downstream of the Transonic Compressor Rotor (65% Design Speed) -----	82
A1. Photographs of Insulator Notch -----	95
A2. Notching Jig for Thermocouple Insulator -----	96



	PAGE
A3. Method for Marking and Breaking Insulators -----	97
A4. Method for Feeding Fine Wires into an Insulator -----	98
A5. Method for Feeding Fine Wires out of an Insulator -----	99
A6. Spotwelding Fine Wires -----	100
A7. Application of Cement to the Insulator -----	101
A8. Adapting 5 mil Wires to the Sensor -----	102
B1. Photograph of Free Jet Apparatus -----	107
B2. Photograph of the Straight Annulus -----	107
B3. Photographs of the Swirl Annulus -----	108
B4. Photographs of the Probe Mounting Box -----	109
B5. Photograph of the Pitch Angle Survey Mount -----	110



## LIST OF TABLES

1.	PNEUMATIC CALIBRATION COEFFICIENTS -----	83
2.	PNEUMATIC CALIBRATION COEFFICIENTS -----	83
3.	ERROR ANALYSIS OF VELOCITY COMPUTATION -----	84
4.	ERROR ANALYSIS OF VELOCITY COMPUTATION -----	85

THE  
JOURNAL OF THE  
ROYAL ANTHROPOLOGICAL INSTITUTE  
OF GREAT BRITAIN AND IRELAND  
VOLUME 100 PART 1 2000  
PUBLISHED BY THE  
CAMBRIDGE UNIVERSITY PRESS

### ACKNOWLEDGMENT

The development and analysis of the probe designed for this paper would not have been possible without the excellent guidance and support of my thesis advisor, Associate Professor R. P. Shreeve. His insight and background knowledge of this research specialty were an invaluable aid in this work.

Secondly, the preparation of experiments, calibration of equipment, instrumentation of the compressor test rig, and the design ideas for support equipment development were outstanding contributions to this work by Mr. J. E. Hammer. His advice and knowledge of experimental techniques were essential ingredients for the success of the probe development.

Finally, the probe could not have been properly constructed without the precision technical expertise of Mr. G. A. Middleton. His miniaturized machinery background was perfectly suited to the development of a reduced scale combination probe of this type.



## I. INTRODUCTION

The transonic compressor rig was designed and built by Dr. M. H. Vavra in the Turbopropulsion Laboratories at the Naval Postgraduate School as part of an effort to obtain a full understanding of the flow within a compressor stage. This work was sponsored by Naval Air Systems Command, Code 310, through the office of Dr. H. J. Mueller. The compressor has been operated to 65 percent of design speed.

Analysis of the flow within the compressor from measurements consists of a data acquisition process and a data reduction process. A significant capability has, in recent years, been developed at the Laboratories in both processes. The development of data reduction equations and associated computer programs for the transonic compressor has been, to a large extent, the work of Dr. R. P. Shreeve [Ref. 1,2]. The results of this work have enabled computer programming of the data reduction from probes that have interrelated calibration equations.

The need for a better understanding of the actual measurements from probes, that is, the data acquisition phase of the process, was realized when it was found that results obtained from two different "calibrated" probes in identical flow conditions produced results which disagreed by as much as ten percent [Ref. 3]. Methods had to be devised for correcting the calibrations that were established for

Die *Phosphorwasserstoff* (Phosphin) wird durch

Phosphor und Wasserstoff bei 200°C. in Gegenwart von

Phosphorwasserstoff (Phosphin) dargestellt.

Phosphorwasserstoff (Phosphin) wird durch

Phosphor und Wasserstoff bei 200°C. in Gegenwart von

Phosphorwasserstoff (Phosphin) dargestellt.

Phosphorwasserstoff (Phosphin) wird durch

Phosphor und Wasserstoff bei 200°C. in Gegenwart von

Phosphorwasserstoff (Phosphin) dargestellt.

Phosphorwasserstoff (Phosphin) wird durch

Phosphor und Wasserstoff bei 200°C. in Gegenwart von

Phosphorwasserstoff (Phosphin) dargestellt.

Phosphorwasserstoff (Phosphin) wird durch

Phosphor und Wasserstoff bei 200°C. in Gegenwart von

Phosphorwasserstoff (Phosphin) dargestellt.

Phosphorwasserstoff (Phosphin) wird durch

Phosphor und Wasserstoff bei 200°C. in Gegenwart von

Phosphorwasserstoff (Phosphin) dargestellt.

Phosphorwasserstoff (Phosphin) wird durch

Phosphor und Wasserstoff bei 200°C. in Gegenwart von

Phosphorwasserstoff (Phosphin) dargestellt.

Phosphorwasserstoff (Phosphin) wird durch

the two probes, and these are reported in reference 3. Further improvements to the calibration procedures have subsequently been made and are reported in Appendix B of this paper.

While the previous efforts successfully produced a method for representing the calibration and correction of pneumatic probes, they did not attempt to solve the probe design problems which were revealed in the process. It was difficult to obtain accurate measurements using probes in the transonic compressor for two reasons. First, the size and geometry of the flow area in the compressor prohibited the use of available combination probes, which had generally been developed for larger machines. Thus, it was not possible to obtain velocity vector and stagnation temperature data from a single survey of the flow region. The available alternatives were to make an additional survey in order to obtain the temperature data or to assume that the stagnation temperature was constant throughout the flow region. The data reduction procedures set forth in reference 3 assumed that the stagnation temperature was constant.

A second problem involved the characteristic behavior resulting from the design of the probes that were available for use in the transonic compressor. The effect of the proximity of a boundary on the indicated pressure at the side ports on a five-hole United Sensor probe, and



particularly on a NASA combination probe, introduced significant errors in the velocity measurements. These considerations suggested that a new probe be designed specifically for the transonic compressor. The requirement was for a probe which would eliminate or reduce the magnitude of the boundary effects, while retaining the ability of measuring the complete velocity vector.

The development of a combination probe incorporating a particular pneumatic sensor geometry, a reduction in size, and a thermocouple sensor for temperature measurements is reported in this paper. The development aspects of the probe are presented in Sections III and IV. The fabrication of a fine wire thermocouple sensor for the probe is detailed in Appendix A. (This section is intended to serve as a manual for the fabrication and replacement of similar thermocouple sensors.) Computer reduction of probe survey measurements, including the development of the equations required to calibrate flow measurements, are described fully in Section IV and Appendix C. Preliminary results from measurements made downstream of the rotor of the transonic compressor are presented in Section V.



## II. THE TRANSONIC COMPRESSOR

### A. DESCRIPTION

A schematic of the transonic compressor test rig is shown in Fig. 1. The test rig consists of an air-turbine drive unit and induction section containing a filter, a throttle, a settling chamber, and a flow measuring nozzle. The air turbine is designed to deliver 450 horsepower at 30,000 RPM with a relative blade tip mach number of 1.5. The compressor flow rate is controlled by a rotating throttle plate (Fig. 1). The inlet of the transonic compressor is designed to contract and to rapidly accelerate the flow in order to generate near uniform conditions, with thin boundary layers, at the rotor face [Ref. 4]. Figure 2 shows the probe mounting arrangement and the layout of the compressor assembly.

Because of efforts directed to developing and installing new instrumentation, and improvements in the compressor hardware for tests at high speeds, the rig was not run for a period of eighteen months. A close examination of the rotor was made prior to the resumption of test rig operations. The examination revealed what appeared to be deteriorating surfaces on the leading edges and the initial flow impact areas on the pressure side of the rotor blades. Nicks and pits on the blade surfaces accompanied by a deposition of whitish material covering small surface flaws



were also detected. Since the rotor had acquired only 120 hours of operating time at speeds up to 65 percent of design, the condition of the rotor required some remedial action.

A complete metallurgical analysis was made on the rotor at the Naval Air Rework Facility, NAS North Island in October 1975. No hairline cracks were detected on the blade surfaces. The rotor was shot-peened and protectively coated to prevent similar deterioration in the future.

#### B. INSTRUMENTATION

The transonic compressor is equipped with stationary probes to measure routine performance data. The case was modified to provide for other probe mountings which will obtain temperature and unsteady flow pressure data. A series of Kiel probes was installed at the stator exit to obtain peripheral impact pressure data. A new honeycomb flow straightener (Fig. 2) was installed to allow a measurement of torque. The flow rates produced as a result of the honeycomb installation were not significantly different from those that were obtained without the flow straightener installed.

The combination probe mounting arrangement is shown in Fig. 2. Radial surveys were made by manually positioning the probe using a traverse unit. An automatic, remotely controlled traverse unit, designed by Lt. D. D. Patton [Ref. 5], will be adapted to the combination probe in future



measurements. Peripheral surveys of the flow were made by manually rotating the outer casing of the compressor assembly. All pressures were measured by a calibrated transducer in a scanivalve arrangement.

#### C. ROTOR PERFORMANCE DETERMINATION USING A COMBINATION PROBE

It is necessary to determine the radial distributions of the flow velocity and angle in order to establish the operating condition and determine the blade element performance. By placing a probe in the flow upstream of the rotor at or near design speeds, the possibility arises that wakes in the flow might induce vibrations in the highly stressed rotor blades. Therefore computations of performance data at these speeds must be based on data obtained at lower speeds. A description of the tests that were made to determine the flow conditions ahead of the rotor at low speeds is presented in Section III of Ref. 3.

The procedures for determining flow conditions downstream of the rotor from probe measurements are given in Section IV of Ref. 3. The only difference in the present work was that stagnation temperature data were recorded on paper tape with the pneumatic data.

The program entitled TCR Reduction (Station 2) [Ref. 3], was modified to incorporate a Mach number calculation for each point in the flow based on the stagnation temperatures that were measured. The program accepted data from the mass memory platter (peripheral part of HP 9830A



calculator system). The paper tape data were therefore entered and transferred to the mass memory before the data reduction program was run. Following reduction, the reduced data were stored on the mass memory platter. Finally, the reduced data were recalled from the mass memory and plotted on the X-Y plotter.



### III. PROBE DESIGN

#### A. DESCRIPTION

A drawing of the combination probe is shown in Fig. 3. The probe consists of four pressure ports which are labelled P1, P2, P3, and P4 (Fig. 3) and a thermocouple sensor which senses a measure of stagnation temperature. The temperature sensor is located 90 mils (0.090 inches) below the pneumatic port where impact pressure (P1) is measured. The probe separates at a point three inches from the sensor tip (Fig. 4). This feature permits the removal and installation of thermocouple sensors from the 0.050 inch O.D. protection tube which houses the sensor. The connector at the upper end of the probe (Figs. 3,4) provides a disconnect feature to remove unnecessary wiring if only pneumatic measurements are required in a specific survey. Figure 5 shows enlarged views of the pressure ports and the section that is immersed in the flow region.

#### B. PNEUMATIC SENSOR DESIGN

Reference 2 states that in principle a multiple sensor pneumatic probe can be calibrated to determine the velocity vector in an unknown flow so long as the measurements taken for a given set of flow conditions are repeatable. It was also shown as a result of an analysis of boundary and interference effects [Ref. 2] that these effects can be greatly reduced if the probe sensors are located forward of the



cylindrical body of the probe. The size of the flow region, and the probe mounting arrangement on the transonic compressor, previously would not allow the use of a wedge or similar probe to measure static pressure in the compressor, to confirm the correction procedure.

Based on these considerations the primary design requirements for the new combination probe were to reduce the size of the probe as much as possible and eliminate or reduce the boundary and interference effects.

Factors limiting the size reduction of the sensor were the strength and probable response of available materials. It was determined that 32 mil stainless steel tubing would meet the durability and size requirement, while continuing to provide acceptable response times to pressure changes.

The size of the stem and the protrusion of the sensors was physically restricted to a circular area  $\frac{1}{4}$  inch in diameter. The probe was to be designed to use the "null-reading" method of determining the flow angle. This requires that the probe be oriented to a position where the same pressure is recorded at two side-port sensing holes ( $P_2=P_3$ ). For a "null-reading" arrangement a sensor geometry is chosen which will produce a pressure response with angle change that is as close to linear as possible. Also, the pressure of the side ports should be lower than the impact pressure by an amount close to the dynamic pressure. Figures 6 and 7 show the results of the tests conducted on 32 mil tubing



to determine the pressure response to pitch and yaw angle changes. From these results it was determined that a 55° bend in the side-port (P2 and P3) and pitch angle (P4) pneumatic stems would meet design requirements and provide negligible interference effects.

A test apparatus (Fig. 8) was set up to determine if the probe characteristics would provide a usable set of calibration curves. Some of the results of the initial runs are shown in Figs. 9, 10, and 11. The tests determined the probe performance as a function of Mach number (velocity for this test) and pitch angle. The probe pressures were measured at nine different velocities (Fig. 9). At each velocity the pitch angle was varied, using the mechanism described in Appendix B, by rotating the probe from -30 to +35 degrees in increments of 5 degrees, keeping the tip at a point in the center of the free jet.

The initial results were good. The impact pressure (P1) agreed with the impact pressure measured by a Prandtl pitot probe except at pitch angles greater than  $\pm 25$  degrees. At these large angles, an interference between the sensors is likely to occur. The results of the measurements (P1-P23) and (P1-P4) plotted against pitch angle for the nine velocities are shown in Figs. 9 and 10. Fig. 11 shows the combination probe calibration function Beta, which is derived in Section IV, as a function of pitch angle, for each of the nine velocities.

...the ... of ...  
...the ... of ...  
...the ... of ...  
...the ... of ...  
...the ... of ...

...the ... of ...  
...the ... of ...  
...the ... of ...  
...the ... of ...  
...the ... of ...

...the ... of ...  
...the ... of ...  
...the ... of ...  
...the ... of ...  
...the ... of ...

...the ... of ...  
...the ... of ...  
...the ... of ...  
...the ... of ...  
...the ... of ...

...the ... of ...  
...the ... of ...  
...the ... of ...  
...the ... of ...  
...the ... of ...

The range of pitch angle to be expected in the transonic compressor is less than  $\pm 20$  degrees. The initial calibration pressure measurements using the combination probe (Figs. 9, 10, 11) clearly showed well behaved smooth curves that could be approximated analytically to allow the reduction of data from the transonic compressor. Section IV describes the probe calibration procedure and results.

### C. THERMOCOUPLE SENSOR DESIGN

#### 1. Background

In incompressible flow, the temperature is considered to be constant throughout the field, and it can be measured sufficiently accurately by means of a sensor sufficiently immersed in the flow. In compressible flow, however, the temperature varies considerably throughout the field; it becomes necessary to distinguish between the temperature which would be recorded by a sensor moving with the fluid (static temperature) and the temperature attained when the fluid is brought to rest adiabatically (stagnation temperature). To measure stagnation temperature it is necessary to bring the fluid to rest and provide some means of measuring the temperature at the stagnation point. A well-designed thermocouple sensor can provide good stagnation temperature measurements. Venting of the thermocouple head is sometimes required, and provision must be made to reduce heat losses by conduction and radiation. Shields are often used in many applications but such devices can also be the source of significant heat losses.



At all speeds, calibration is necessary. The characteristics of the instrument can be conveniently expressed in the form of a "recovery factor" defined as

$$r = (T_p - T)/(T_t - T)$$

where  $T$  is the free stream static temperature,  $T_p$  is the temperature recorded by the thermocouple, and  $T_t$  is the stagnation temperature. A recovery factor of 1.0 is optimum. As reported in Ref. 6, the major difficulty in using standard probe designs is that the recovery factor depends on Reynolds Number, Mach number, and total temperature in certain ranges of parameters. The study reported in Ref. 6 determined that recovery factors near 1.0 could be attained by simply miniaturizing an unshielded thermocouple probe. In particular, it was found that the thermocouple wire must be very small relative to the size of the stagnation region in which the thermocouple is immersed. The study also indicated that a concave tip for the sensor might provide a more effective stagnation region over a range of flow angles.

Stagnation temperatures in the transonic compressor are low; consequently conduction losses are the largest potential source of error. This suggested that the swage type of thermocouple construction be avoided in the design of the sensor. The use of a glassy nonconductive insulator for housing the thermocouple required a special design but was preferred.



In summary then, the main requirements for the thermocouple sensor design were:

1. The size of the thermocouple and wire should be small.
2. The probe should be unshielded.
3. A geometry creating a large stagnation region relative to the wire size over a wide range of pitch angles should be determined.
4. A nonconducting, insulating material which could be machined to a specific geometry should be used.

Based on the above requirements, the components chosen for the thermocouple sensor were a 1 mil fine-wire chromel-constantan thermocouple (good performance qualities in the low temperature range, and durable) and a 32 mil, two-hole alumina insulator. Two basic geometries were tested. The characteristics and test results of each design are reported in the following two parts of this Section.

## 2. Initial Design and Test Results

Figure 12 shows a schematic of the initial thermocouple probe geometry. Figure 13 shows the geometry of the 50 mil protection tube which housed the thermocouple sensor as a part of the combination probe.

Doubts were expressed regarding the suitability of this design from its inception. Fabrication and testing were carried out, however, because the design was simple to fabricate and the benefit of the ruggedness of the design warranted the attempt.



A test was conducted using two temperature probes of this design to determine the sensitivity of one of them to pitch angle and Mach number in a free jet. The test apparatus is shown in Fig. 8. The results of this test (Fig. 14) clearly indicated the sensitivity of the design to both pitch angle and Mach number.

These characteristics were unacceptable, although the data indicated that at a pitch angle of just  $-15^\circ$  the geometry was such that a temperature measurement which was insensitive to Mach number could be achieved. The results suggested that a stagnation region did not exist around the thermocouple sensor except in a very limited set of conditions. It was suspected that the bleed hole on the aft side of the protection tube (Fig. 13) was too large, although subsequent tests with the hole plugged were inconclusive. The sides of the 50 mil tube encasing the sensor were suspected to have introduced large heat conduction losses at pitch angles greater than  $-10^\circ$  relative to the flow because of their proximity to the thermocouple head.

### 3. Final Design and Test Results

The results of the initial thermocouple design indicated that a stagnation region probably did not exist around the thermocouple head except at a pitch angle near  $-15^\circ$ . Also, the metal tubing that housed the insulator was suspected of introducing conductive heat losses which varied with both Mach number and pitch angle. The final thermocouple design attempted to overcome these problems by making



the following changes. First, a small notch was made in the insulator to produce a stagnation region that would be more insensitive to pitch angle changes in the flow (Figs. 15, 16). The concave notch follows the suggestion made in reference 6. Secondly, the stainless steel tubing supporting the insulator was machined to significantly reduce the amount of metal that could absorb, and conduct away, heat from the flow in the region of the temperature measurement (Figs. 5, 15).

The resulting geometry of the sensor is shown in Fig. 15. This design provides poorer protection from mishandling than the initial design (Fig. 12). However, the durability of the sensor itself in the flow was found to be excellent. No failures have been experienced while testing, but care must be taken when storing the probe and attaching it to test apparatus.

A test to determine the sensitivity of the probe to pitch angle and Mach number was conducted so that a comparison could be made between the first and second probe geometries. The results of the test are shown in Fig. 17. A comparison of these data with the data shown in Fig. 14 shows considerable improvement in the performance of the second design.

The primary application of the probe is for conditions where the pitch angle varies from 0 to +20 degrees. Figure 17 shows little or no pitch angle effect on the probe



for this range of pitch angles, and the effect of Mach number has been greatly reduced from that of the first design. The Mach number effects that do exist were accounted for in the calibration of the sensor.

The above results indicated that the second design could be calibrated to provide an accurate measure of total temperature for the probe at pitch angles from 0 to +20 degrees and for Mach numbers from 0 to 1.0. The calibration of the thermocouple sensor is described in Section IV. A method for the fabrication of the final design is presented in Appendix A.



#### IV. PROBE CALIBRATION TEST RESULTS

##### A. METHOD OF APPROACH

The limited axial space available for instrumentation in most turbomachinery flow passages severely limits the types and sizes of probes which can be used. The combination probe was designed to be used for surveys between the rotor and the stator of the transonic compressor (Fig. 2). The probe, when calibrated, measures flow velocity, yaw angle, pitch angle, and total temperature. The method of calibration presented here is based on the method given in Appendix A of Ref. 3.

The probe calibration data were obtained in tests using the free jet (4.2 inch diameter) nozzle described in Appendix B. The data were reduced to polynomial expressions which represented the pitch angle, flow velocity, and total temperature that was measured by the probe. In application, the polynomial expressions are used to reduce the pressures and voltage registered by the probe to values for the pitch angle, velocity, and total temperature.

It is important to note that the calibration for the combination probe was carried out only in the free jet. It is recommended that further measurements be made in the straight annulus and swirl annulus (Appendix B) to determine the wall effects, immersion effects, and blockage effects of the probe on the free jet calibration results. The free



jet calibration of the combination probe was carried out for a range of pitch angles between 0 and +20 degrees and a range of Mach numbers between 0 and 1.0. This variation in parameters spanned the range of conditions that have been determined to exist in the flow passages of the transonic compressor to date.

#### B. THE PNEUMATIC CALIBRATION

The readings of the probe depend on flow Mach number. It is more convenient, however, to non-dimensionalize the velocity using the "limiting" velocity,  $V_t = (2C_p T_t)^{1/2}$  (for a perfect gas). Use of the limiting velocity is discussed in Appendix A of Ref. 1. The non-dimensionalized velocity is given by

$$X = (V/V_t) \quad (1)$$

where  $V_t = 109.62(T_t)^{1/2}$  ft/sec. for air when the stagnation temperature  $T_t$  is in °R. References 1 and 2 give the relationships between static and stagnation gas properties which are

$$\begin{aligned} T/T_t &= 1 - X^2 \\ p/p_t &= (1 - X^2)^{\gamma/1-\gamma} \\ \rho/\rho_t &= (1 - X^2)^{1/\gamma-1} \end{aligned} \quad (2)$$



The relationship between Mach number and X is given by

$$X = ((\gamma-1)/2)M^2 / (1+(\gamma-1)/2)M^2 \quad (3)$$

The calibration of the pneumatic part of the combination probe can be represented in the form of two functions of Mach number (or X) and pitch angle  $\phi$ . Define

$$\text{Beta} = \beta(X, \phi) = (P_1 - P_{23})/P_1 \quad (4)$$

and

$$\text{Gamma} = \gamma(X, \phi) = (P_1 - P_4)/(P_1 - P_{23}) \quad (5)$$

to be the required calibration functions, where it is understood that the probe pressures are taken when  $P_2 = P_3$ .

To calibrate, the probe was placed in the flow at a known pitch angle and the true impact pressure was measured by a reference probe. The true static pressure was taken to be atmospheric pressure since data were obtained from the free jet apparatus shown in Fig. 8. Data were taken for eleven pitch angles ( $-20^\circ$ ,  $-16^\circ$ ,  $-12^\circ$ ,  $-8^\circ$ ,  $-4^\circ$ ,  $0^\circ$ ,  $4^\circ$ ,  $8^\circ$ ,  $12^\circ$ ,  $16^\circ$ ,  $20^\circ$ ) at the nine Mach numbers (or X's) given in Fig. 18.

The value of X was obtained from true static and stagnation pressures using Eq. (2) giving, for the case where the static pressure is atmospheric,



$$X = (1 - (1/\gamma)((Pr - Pa)/Pa) + 1)^{\gamma - 1/\gamma} \gamma^{1/2} \quad (6)$$

where  $Pa$  = atmospheric pressure, and  $Pr$  = reference (true) stagnation pressure. The value of  $X$  was calculated from Eq. (6) and the values of  $\beta$  and  $\gamma$  from Eq. (4) and Eq. (5).

The data were plotted in graphical form as follows:

$\beta$  vs.  $\phi$                       for constant  $X$

$\gamma$  vs.  $\phi$                       for constant  $X$

$X$  vs.  $\beta$                       for constant  $\phi$

The data points were fit by a fifth order polynomial curve using the Hewlett-Packard 9830A calculator and X-Y plotter. The plot and polynomial curve fits for each set of data are shown in Figs. 18, 19, and 20. The polynomial curve fit for each set of data points gave six coefficients for each curve. Thus for each  $\gamma$  vs.  $\phi$  plot (Fig. 19) the six coefficients  $A_0, A_1, \dots, A_5$  were calculated for the polynomial expression for  $\gamma$  as a function of  $\phi$ :

$$\gamma = A_0 + A_1\phi + A_2\phi^2 + A_3\phi^3 + A_4\phi^4 + A_5\phi^5 \quad (7)$$

at each value of  $X$ .

The same procedure was applied to the  $X$  vs.  $\beta$  data (Fig. 20) to derive a polynomial expression for  $X$  as a



function of  $\beta$ ;

$$X = B_0 + B_1\beta + B_2\beta^2 + B_3\beta^3 + B_4\beta^4 + B_5\beta^5 \quad (8)$$

The curves developed in Fig. 18 were not in a form that could be used as a calibration. From Fig. 19 nine expressions for  $\gamma$  (Eq. (7)) were obtained (one for each value of  $X$ ) and from Fig. 20 eleven expressions for  $X$  (Eq. (8)) were obtained (one for each value of  $\phi$ ).

A further reduction was necessary to develop a single polynomial expression for  $\gamma$  and a single polynomial expression for  $X$ . The two complete expressions would represent an analytical approximation of the calibration data from which  $X$  and  $\phi$  could be obtained by iteration when  $\beta$  and  $\gamma$  were known from measurements.

To obtain a manageable number of coefficients, the following reduction was made. The coefficients derived from the curves in Fig. 19 were plotted against each  $X$  as follows:

A0(I) vs. X(I)	-----	9 points
A1(I) vs. X(I)	-----	9 points
.		
.		
.		
.		
A5(I) vs. X(I)	-----	9 points



This produced curves of the form

$$\begin{aligned}
 A_0 &= a_0 + a_1x + a_2x^2 + a_3x^3 \\
 A_1 &= a_0^1 + a_1^1x + a_2^1x^2 + a_3^1x^3 \\
 &\vdots \\
 A_3 &= a_0^3 + a_1^3x + a_2^3x^2 + a_3^3x^3
 \end{aligned}
 \tag{9}$$

which resulted from a third order polynomial curve fit as shown in Fig. 21. (Or, equivalently, fifth order in which the coefficients of the fourth and fifth order terms became zero.)

The coefficients from Fig. 20 were plotted against each

$\phi$

B0 vs. $\phi$	-----	11 points
B1 vs. $\phi$	-----	11 points
.		
.		
.		
B3 vs. $\phi$	-----	11 points

giving values for the coefficients of a third order polynomial curve fit of the form



$$\begin{aligned}
B_0 &= b_0 + b_1\phi + b_2\phi^2 + b_3\phi^3 \\
B_1 &= b_0^1 + b_1^1\phi + b_2^1\phi^2 + b_3^1\phi^3 \\
&\vdots \\
B_3 &= b_0^3 + b_1^3\phi + b_2^3\phi^2 + b_3^3\phi^3
\end{aligned} \tag{10}$$

(Equivalently, the fourth and fifth order coefficients became zero.)

The curves represented by Eq. (10) are shown in Figs. 22, 23, 24, 25, 26, 27. With the  $A_0, A_1, A_2, \dots, A_5$  coefficients written as in Eq. (9) the equation for  $\gamma$  becomes

$$\begin{aligned}
\gamma &= (a_0 + a_1X + a_2X^2 + a_3X^3 + a_4X^4 + a_5X^5) + \\
&(a_0^1 + a_1^1X + a_2^1X^2 + a_3^1X^3 + a_4^1X^4 + a_5^1X^5)\phi + \dots \\
&\dots + (a_0^5 + a_1^5X + a_2^5X^2 + a_3^5X^3 + a_4^5X^4 + a_5^5X^5)\phi^5
\end{aligned} \tag{11}$$

Similarly with the coefficients  $B_0, B_1, B_2, \dots, B_5$ , written as in Eq. (10) the equation for  $X$  becomes

$$\begin{aligned}
X &= (b_0 + b_1\phi + b_2\phi^2 + b_3\phi^3 + b_4\phi^4 + b_5\phi^5) + \\
&(b_0^1 + b_1^1\phi + b_2^1\phi^2 + b_3^1\phi^3 + b_4^1\phi^4 + b_5^1\phi^5)\beta + \dots \\
&\dots + (b_0^5 + b_1^5\phi + b_2^5\phi^2 + b_3^5\phi^3 + b_4^5\phi^4 + b_5^5\phi^5)\beta^5
\end{aligned} \tag{12}$$



This procedure resulted in a single equation (Eq. (11)) for  $\gamma$  in which the coefficients were analytic functions of  $X$ , and a single equation for  $X$  (Eq. (12)) in which the coefficients were analytic functions of  $\phi$ . The coefficients for these expressions are given in Tables 1 and 2. The equations and coefficients were programmed into a general reduction program entitled REPROO.

The calibration data from which the coefficients were derived were fed into the program and  $X$  and  $\phi$  were calculated. The curves that are represented by Eqs. (11) and (12) with the coefficients given in Tables 1 and 2 are plotted with the data points in Fig. 28.

The results show good accuracy for values of  $X$  from 0 to 0.30 at all pitch angles and for values of  $X$  from 0 to 0.38 at pitch angles from  $-4$  to  $+20$  degrees. Within these limits the calculation of  $\phi$  was made to within 0.5 degrees of the actual value in all but six instances.  $X$  was calculated using Eq. (11) and Eq. (12) and the values compared with the actual values of  $X$ . These results are shown in Table 3. In most cases the error was less than one percent.

In an additional test a survey was made of the free jet using the combination probe. This allowed an additional determination of the accuracy of  $X$  with data other than the data which were used to develop the calibration. Fig. 29 shows a comparison of the velocity profiles calculated from impact pressure and atmospheric static pressure, with



the profile derived from an application of the probe calibration to the probe measurement. Table 2 gives an error comparison for these data. The results show disagreement as large as 2.95 percent between the two velocity profiles. A comparison with the results from Table 3 indicated that an error of less than one percent was expected. The reason for the disagreement is not known. Since the data were recorded in different runs, a small leak in the measuring apparatus might have developed, and therefore the measurements must be repeated. This problem is discussed in Section V.

#### C. THE THERMOCOUPLE CALIBRATION

The thermocouple was calibrated in an oil bath with reference to the reference thermocouple probe in an ice bath to establish accurately the relationship between the known temperature difference and the thermoelectric voltage produced by the 1 mil chromel-constantan thermocouples. Data points were collected in the temperature range from 32 - 200 °F. The data were plotted, approximated by a polynomial and compared with the calibration data supplied by the thermocouple manufacturer. Figure 30 shows the data points with a second order curve fit by polynomial regression. The temperature coefficients  $A_0$ ,  $A_1$ , and  $A_2$  obtained are shown in Fig. 30.

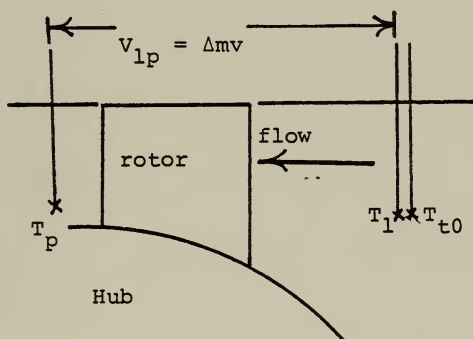
The calibration curve established a relationship between the probe temperature in °F ( $T_p$ ) and the thermoelectric



voltage in millivolts, (V), in the form

$$T_p = A_0 + A_1V + A_2V^2 \quad (13)$$

In the transonic compressor, the reference stagnation temperature ( $T_{t0}$ ) is measured in the flow upstream of the rotor as shown below.  $V_{lp}$  is a measure of the emf generated between  $T_{t0}$  and the thermocouple sensor in millivolts. Since  $T_{t0}$  is known from a separate iron-constantan thermocouple probe interpolation of Fig. 30 using Eq. (13) gives a value for the thermoelectric voltage ( $V_1$ ) corresponding to the known reference temperature.



Define  $V_p$  as the thermoelectric voltage that represents the stagnation temperature at the probe.



$$V_p = V_1 + V_{1p} \quad (14)$$

Since  $V_{1p}$  is measured and  $V_1$  is known from Eq. (13), then  $V_p$  and thus  $T_p$  is determined.

The probe temperature ( $T_p$ ) for a given stagnation temperature ( $T_t$ ) was found to depend slightly on Mach number. The recovery factor was defined (Section III.C.) as

$$r = (T_p - T)/(T_t - T) \quad (15)$$

where  $T_p$  is the static temperature. In terms of  $X$  Eq. (15) becomes

$$T_p/T_t = 1 - (1-r) X^2$$

or, equivalently

$$(T_t - T_p)/T_t = (1-r) X^2$$

Since the recovery factor depends on  $X$ , the probe calibration data were plotted to establish the probe error in the form

$$F_t(X^2) = (T_t - T_p)/T_t = C_0 + C_1X + C_2X^2 \quad (16)$$



Eq. (16) gives a value for the correction to be applied to the probe measurement as a function of Mach number in the form of a polynomial expression. To obtain the coefficients in Eq. (16), the recovery factor  $((T_t - T_p)/T_t)$  measured in the calibration tests was plotted vs.  $X$  for all pitch angles and for eight Mach numbers (Fig. 31). The calibration data for values of  $\phi$  from 0 to  $20^\circ$  were used. This was representative of the range of pitch angles seen by the probe in the transonic compressor. An average value for the recovery factor at each Mach number was calculated for this range of  $\phi$  and plotted vs.  $X$  (Fig. 32). The values were then approximated by a second order polynomial so that the coefficients in Eq. (16) were evaluated.

A subroutine DODGE9 was developed and incorporated into the first compressor reduction program REPRO1 to determine the probe temp  $(T_p)$  from measurements of  $T_{p0}$  and  $V_{1p}$  using Eq. (13) and Eq. (14). A second subroutine was incorporated in the second compressor reduction program REPRO2 to calculate the stagnation temperature  $(T_t)$  from the probe temperature and the measured value of  $X$  using Eq. (16). From  $T_t$  and  $T_{t0}$ , the non-dimensional temperature rise across the rotor  $(T_t - T_{t0})/T_{t0}$  was calculated and plotted.



## V. APPLICATION IN THE TRANSONIC COMPRESSOR

The new combination probe and the United Sensor Corporation probe which was used for the study reported in Ref. 3, were mounted on the transonic compressor to perform radial surveys at the exit of the rotor. The two probes were displaced  $120^\circ$ , peripherally. In compressor tests at two speeds (50 percent and 65 percent of design speed), the probes were simultaneously traversed radially inwards in increments of 0.1 inches. At each point, the two probes were rotated to balance the side port pressures and the yaw angle and linear displacement were recorded. Also, all probe pressures, thermocouple differential voltage, and compressor reference data were automatically recorded by the steady-state data system [Ref. 4] on paper tape. Pressures were measured to an accuracy of 0.1 inches of water using a Scanivalve referenced to atmospheric pressure. The combination probe data were reduced using the pneumatic and thermocouple calibrations described in Section IV, using computer programs listed in Appendix C. The results were plotted using the programs developed in Ref. 3, and are compared with data previously obtained from a NASA combination probe at similar compressor conditions in Figs. 33-36. The data obtained from the 5-hole probe were not reduced, however, Fig. 18 and Fig. 20 of Ref. 3 show data from the 5-hole probe obtained at similar compressor conditions.



The following observations are made as a preliminary appraisal of the results shown in Figs. 33-36.

1. The stagnation temperature rise measured by the new combination probe agrees extremely well with the earlier measurements using the NASA probe. It should be noted here that the NASA probe was not independently calibrated. A standard calibration for this type of probe was used. The differences at the higher speed (Fig. 35) can be explained by the difference in the flow rate for the two tests.
2. The total pressure rise measured by the combination probe is larger than was previously measured by the NASA probe, and the amount of the difference increases with speed.
3. The results for temperature rise and pressure rise combine to give negative values for the rotor loss coefficient shown in Fig. 34 and Fig. 36. The loss coefficient ( $\zeta$ ) is defined here as  $\zeta = 1 - \eta_r$ , where  $\eta_r$  is the thermodynamic efficiency). If the temperature rise is correct, it appears that the total pressure rise is too high. A preliminary conclusion is that the construction of the probe from straight tubing leads to a different behavior in the periodic flow from the rotor; but this must be confirmed.
4. The differences in the yaw angle measurements of the two probes is seen to be almost constant from hub to tip. It is possible that there was an error in mounting the combination probe with respect to the angle scale. The



larger difference at the higher speed might again result from the difference in flow rate for the two tests.

5. In comparing the distributions of Mach number, it should be noted that the combination probe data were not corrected for boundary effects. Indeed, no investigation has yet been made of the effects of boundaries on the calibration of the probe. The NASA probe data shown in Figs. 18 and 20 of Ref. 3 were corrected for boundary effects. After the corrections were applied, the distributions of Mach number from the NASA and 5-hole probes agreed well over the outer half of the radial distribution. The Mach number from the combination probe is lower in this region. It is possible that some correction might be necessary to the combination probe free-flow calibration for application in the compressor passage [Ref. 2]. It is noted however that there were differences between the present tests and the tests reported in Ref. 3 in how the surveys were conducted, and in the total probe blockage present during the survey. A comparison with the 5-hole probe data taken in the present tests should resolve this question.

The distribution of Mach number over the inner half of the radial distribution agrees well in both shape and magnitude with the 5-hole probe results given in Figs. 18 and 20 of Ref. 3. In Ref. 3 it was noted that the 5-hole probe and NASA probe disagreed in this



region. It was also noted that the radial distribution of static pressure derived from the probe measurements tended to the value measured at the hub wall for the 5-hole probe, but not for the NASA probe. Thus the combination probe measurements, and the wall static pressure measurements are in good agreement over the inner half of the compressor passage.



## VI. CONCLUSIONS

The preliminary results from the application of the combination probe in the transonic compressor were encouraging. These results were discussed in Section V. A more complete assessment will be made when the data taken from the 5-hole probe are reduced.

Further calibration tests should be made in order to improve the present pneumatic calibration and to obtain corrections to the calibration from measurements in the straight annulus and in the swirl annulus. A goal for the pneumatic calibration of the probe is an accuracy in the measurement of  $X$  to within 0.2 percent of the actual value and a measurement of  $\phi$  to within 0.5 percent of the actual value.

The results of the free-jet survey, when reduced using the probe calibration (Fig. 29, Table 4), disagreed with the expected velocities by as much as 2.96 percent. Since the probe was disconnected from the free jet apparatus between the calibration test and the free-jet survey (Dodge Survey #3), the possibility of an undetected leak in either test can not be ignored. It is recommended that the free jet survey be repeated. If the disagreement is repeated, then the calibration must be improved.

To improve the present calibration two steps should be taken. First, repeat the steps that were taken to obtain



the coefficients that were derived from the plots of  $X$  vs.  $\beta$ . The coefficients are shown plotted as functions of  $\phi$  in Figs. 22-27. The third order curve fit that was made for these points smoothed the scatter in the actual values which were derived from data. If a review of the steps to obtain these coefficients produces no change, then a second set of calibration data should be obtained and reduced for conditions comparable to the initial set. This may provide a more accurate determination of the coefficients, which would then change the final coefficients for Eqs. (11) and (12). It is important to note that only very small changes in the values of the final coefficients can significantly affect the accuracy of the calibration.

The calibration of the thermocouple sensor provided an accurate measure of total temperature at the probe. The present calibration contains a small but measurable Mach number effect that is shown in Fig. 17. It is recommended that a  $\frac{1}{2}$ -mil chromel-constantan thermocouple be installed in the probe when the present sensor (1-mil thermocouple) is replaced. This change will effectively double the size of the stagnation region surrounding the thermocouple sensor. The result should be a reduction in the Mach number and pitch angle effects that are present in the current probe design.

In conclusion, the combination probe reported here is a significant advance over the NASA probe in the specific

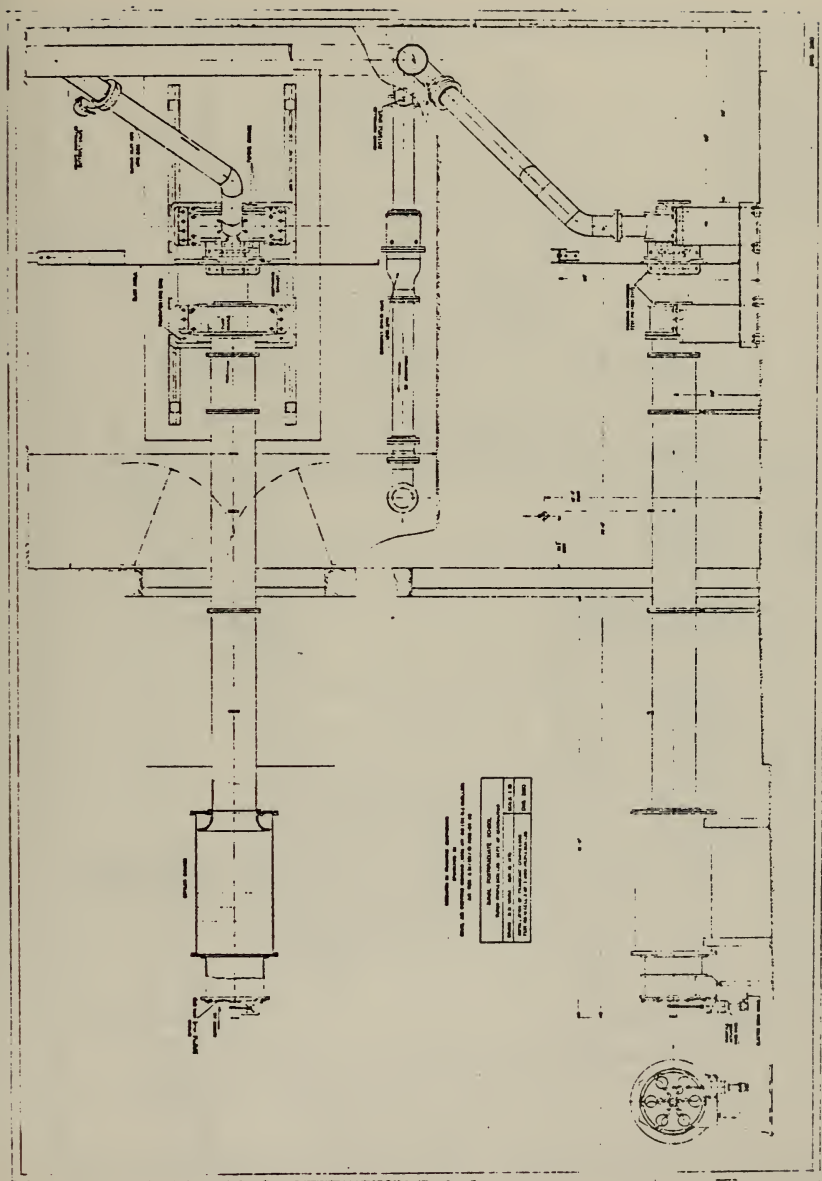


application for which it was developed:

- (i) It is more slender, causing less blockage
- (ii) It provides a measure of the pitch angle
- (iii) The temperature measurement is less sensitive to Mach number
- (iv) The thermocouple sensor can readily be repaired.

The effect of flow boundaries has yet to be measured.















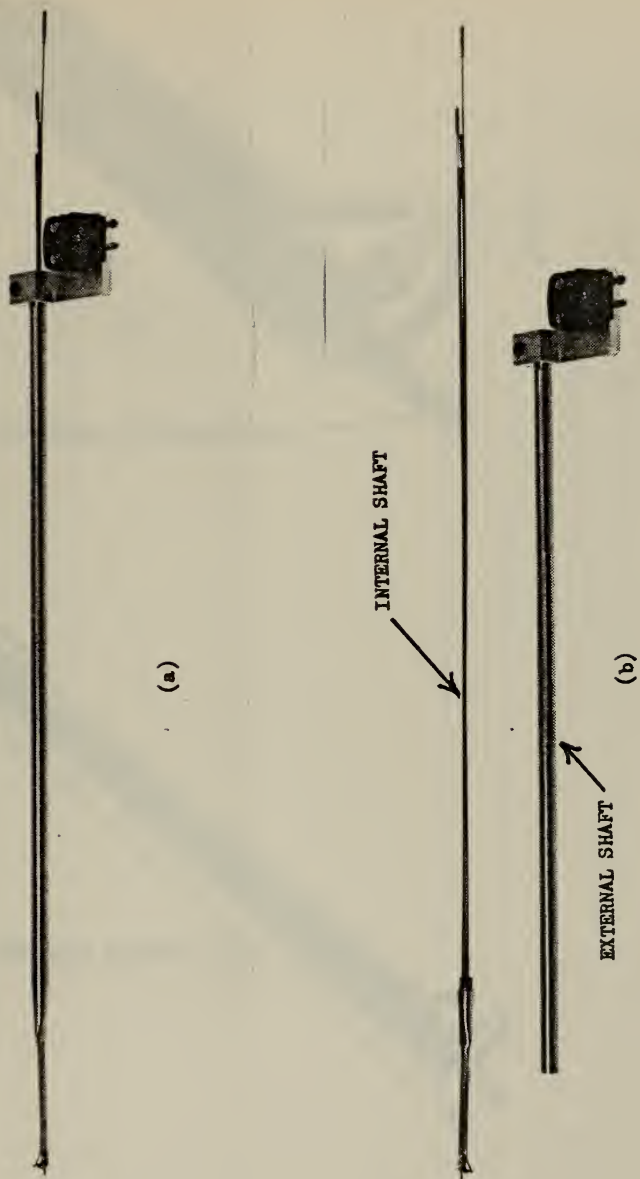


FIG. 4. COMBINATION PROBE (a) CONNECTED (b) SEPARATED



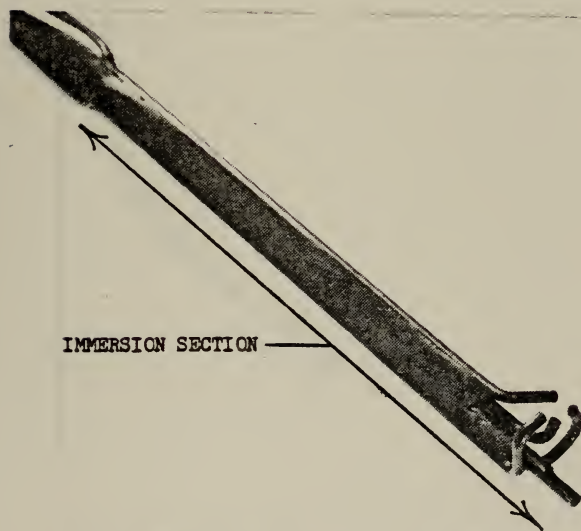
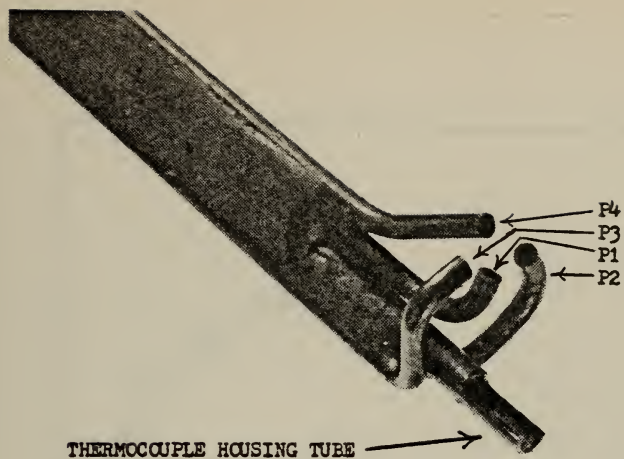


FIG. 5. PNEUMATIC SENSOR TIP WITHOUT THERMOCOUPLE INSTALLED.



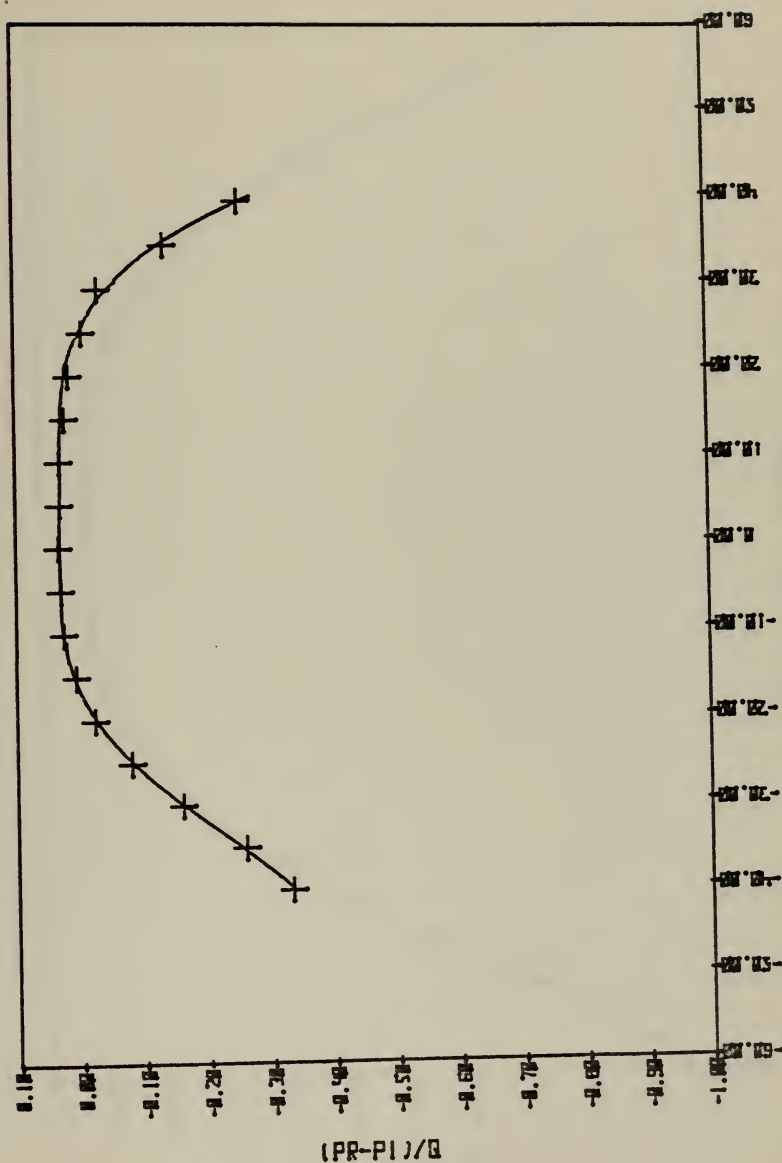


FIG. 6. PITCH ANGLE SENSITIVITY OF A 0.032" TUBE IN A FREE JET



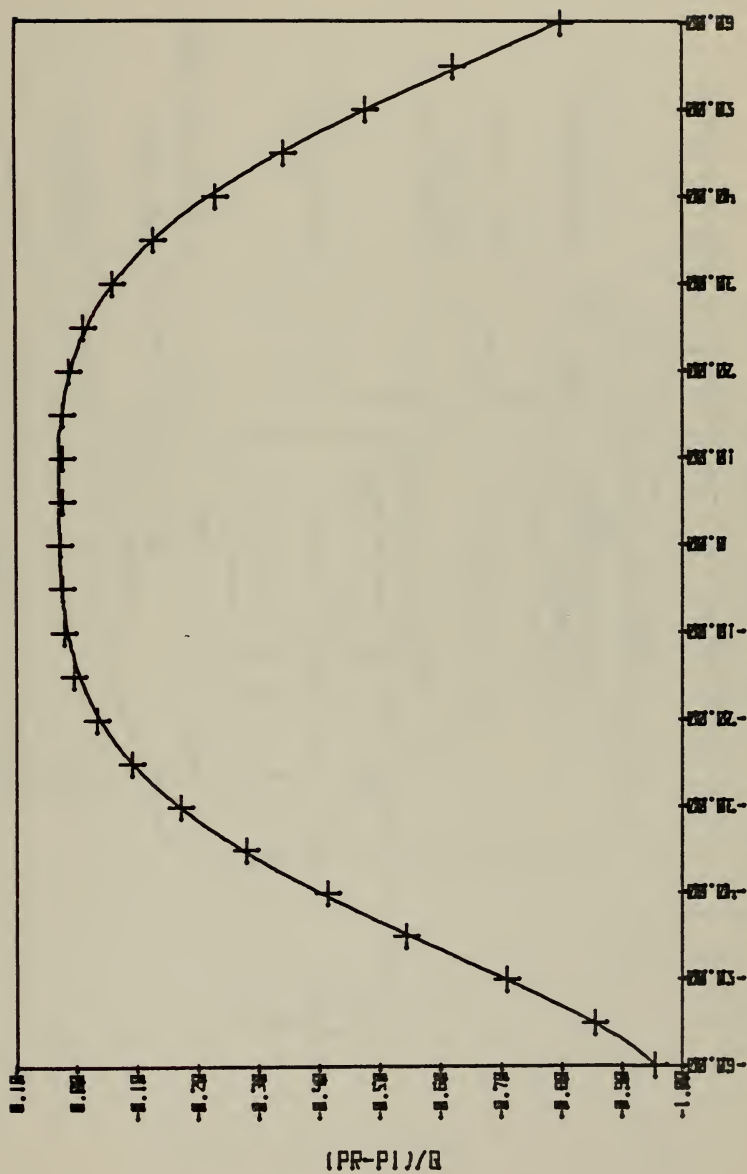


FIG. 7. YAW ANGLE SENSITIVITY OF A 0.032" TUBE IN A FREE JET.



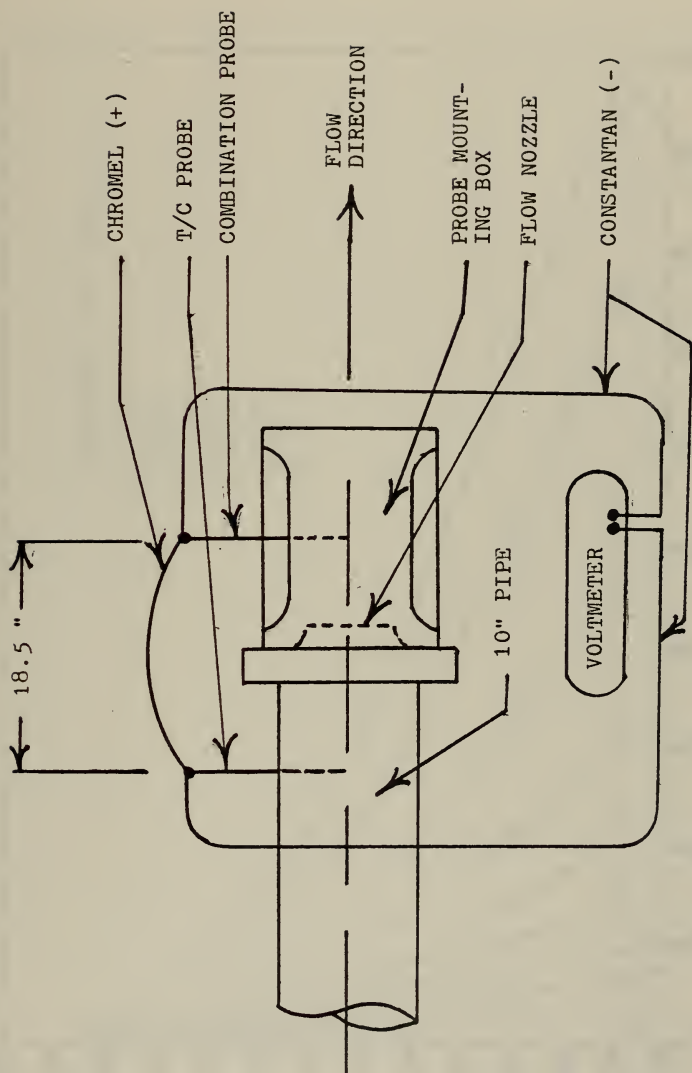


FIG. 8 . THERMOCOUPLE SENSOR AND COMBINATION PROBE TEST APPARATUS .



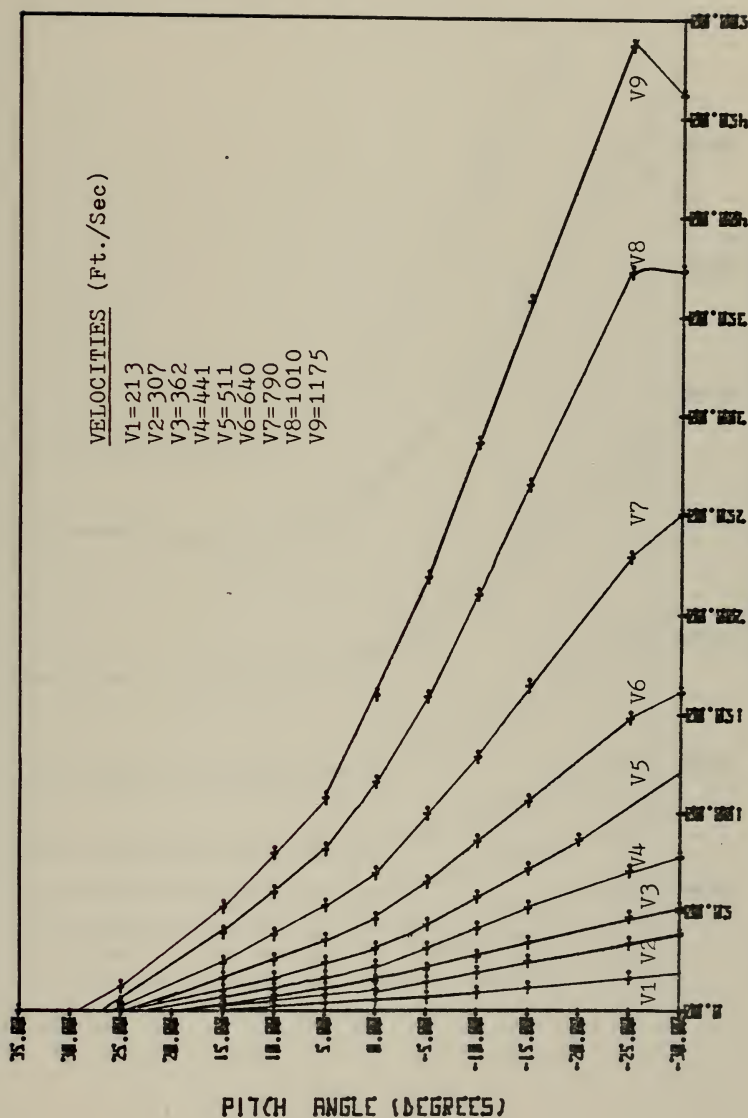


FIG. 9. (P1-P4) VS. PITCH ANGLE FOR NINE VELOCITIES.





FIG. 10 . (PI-P23) VS. PITCH ANGLE FOR NINE VELOCITIES.



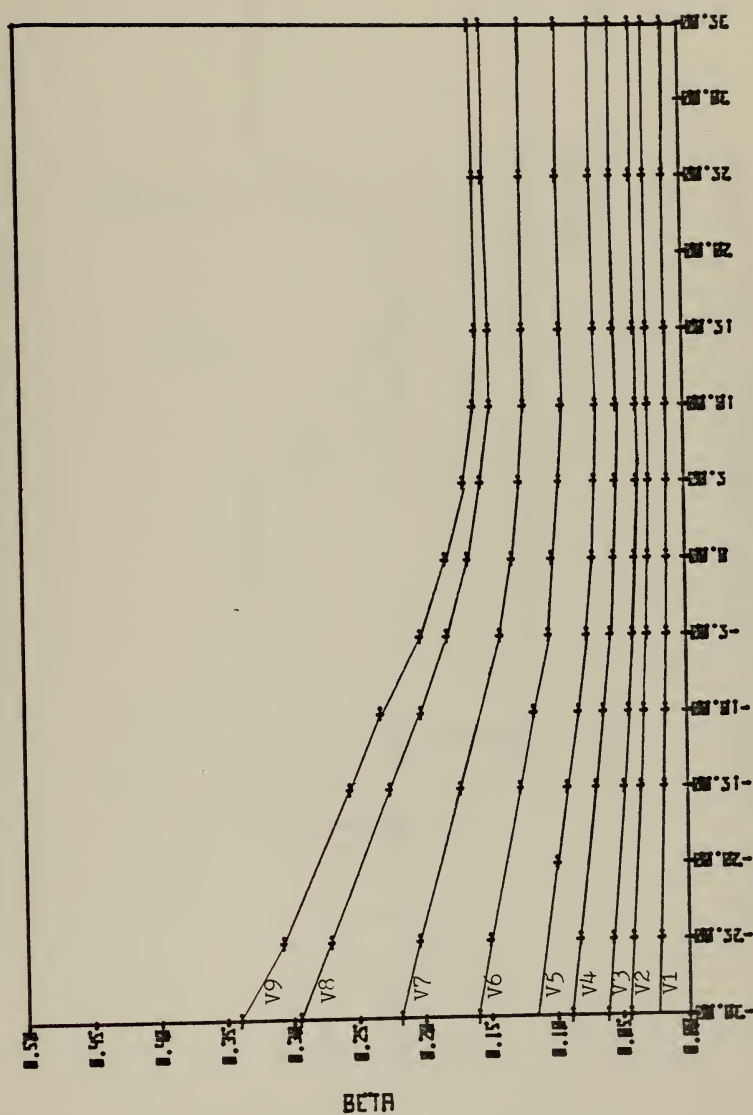


FIG. 11. PITCH ANGLE VS. BETA. INITIAL PROBE SURVEY IN A FREE JET (9 VELOCITIES).



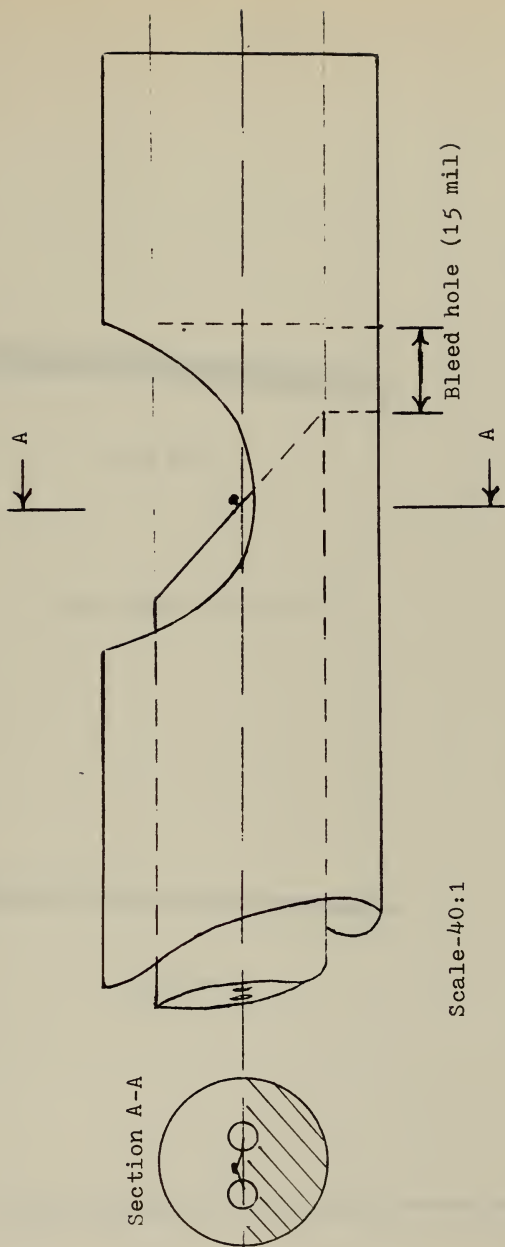
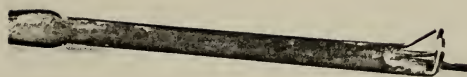


FIG. 12. SCHEMATIC OF INITIAL THERMOCOUPLE PROBE GEOMETRY





Side view

Thermocouple housing tube



Top view

Fig. 13. Initial geometry for thermocouple housing tube.



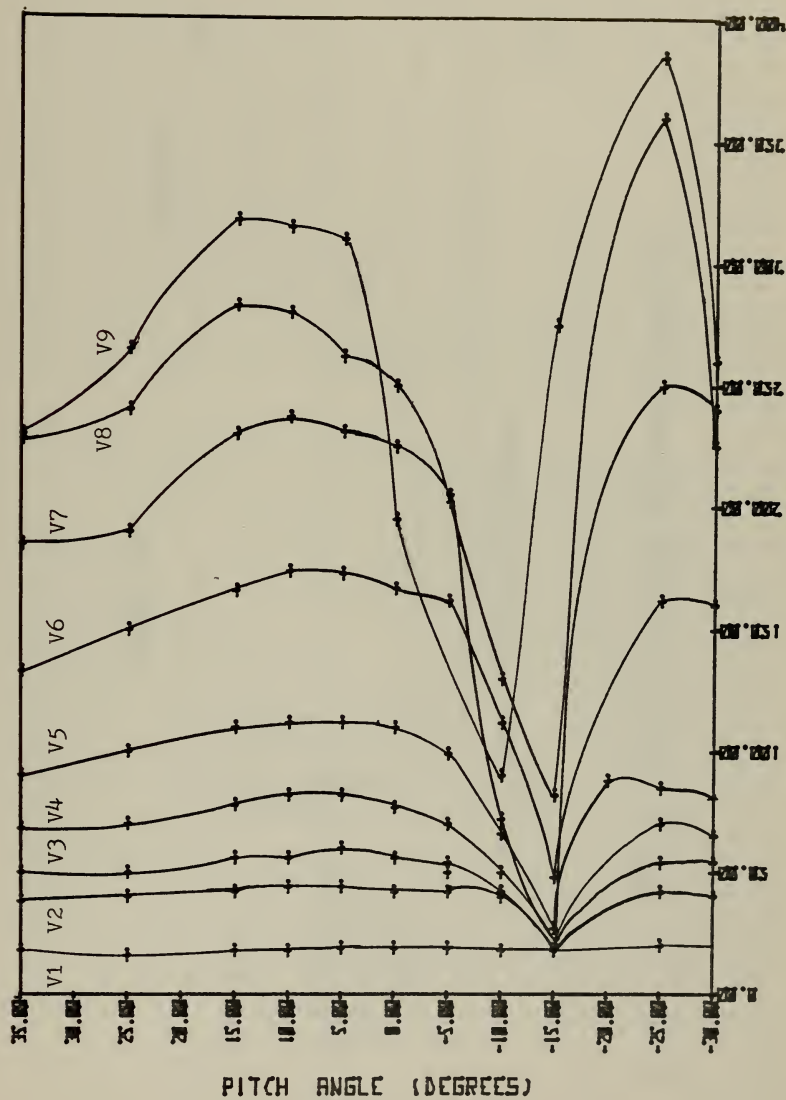


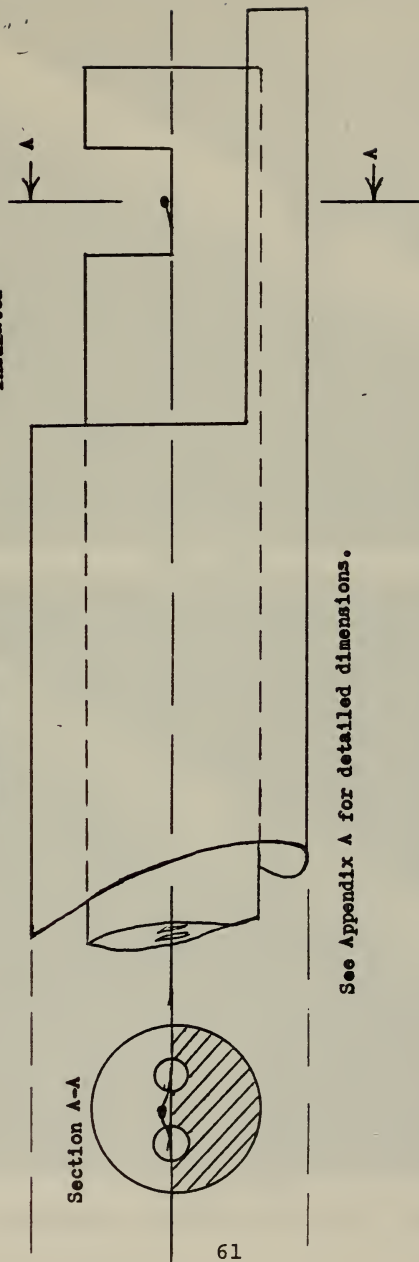
FIG. 14. INITIAL T/C DESIGN. TEMP. VARIATION AS A FUNCTION OF VELOCITY & PHI.



Housing tube

Insulator

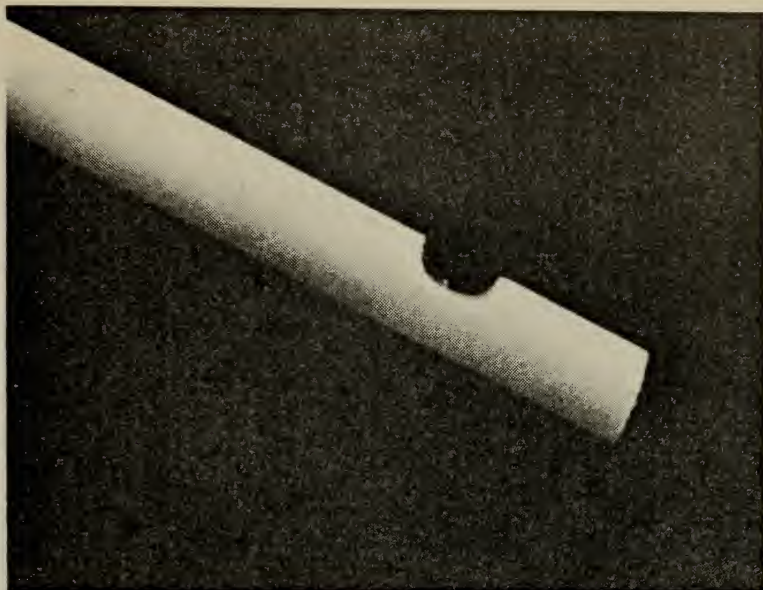
Section A-A



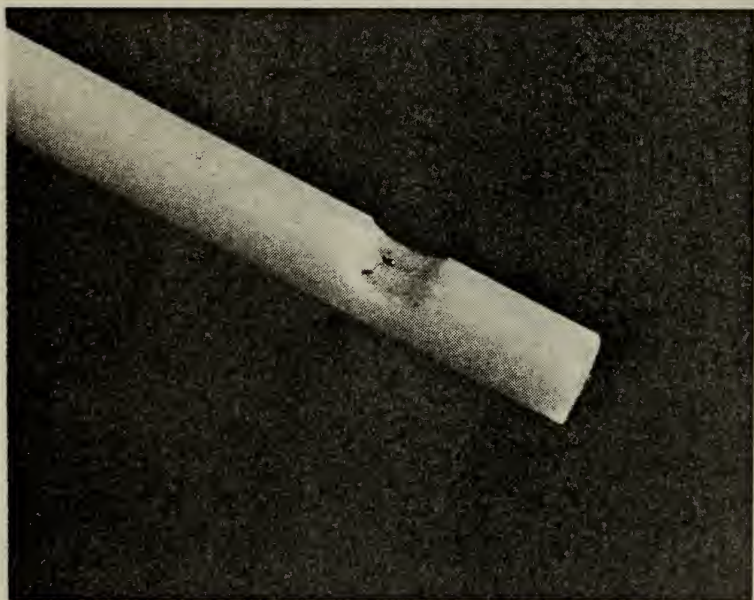
See Appendix A for detailed dimensions.

FIG. 15. Schematic of the final thermocouple sensor design.





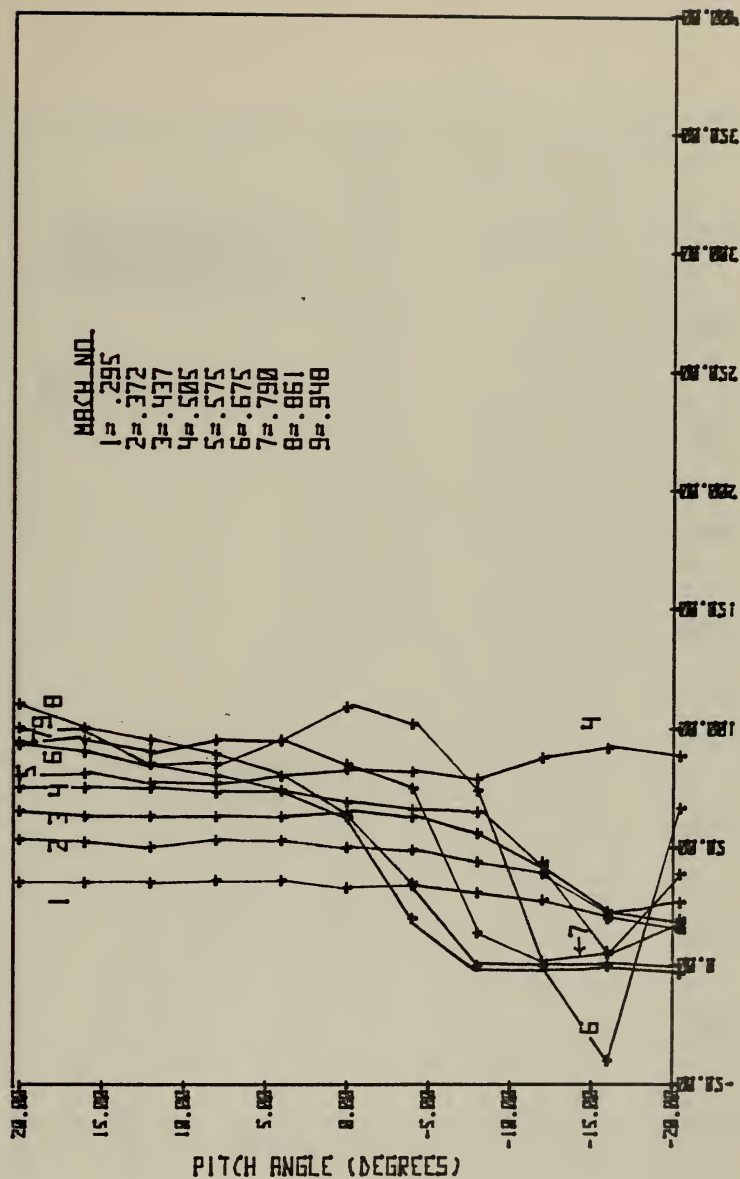
Side view



Oblique view

FIG. 16. Photographs of insulator notch with thermocouple installed.







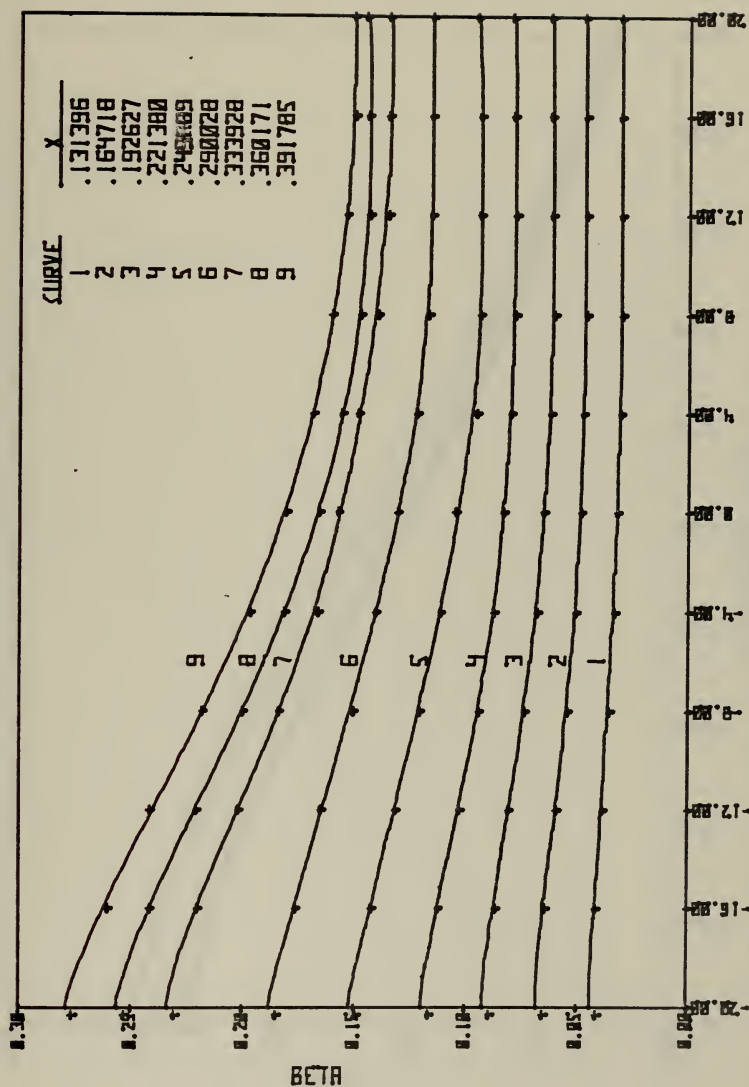


FIG. 18. BETA VS. PHI DATA POINTS AND POLYNOMIAL CURVE FITS.



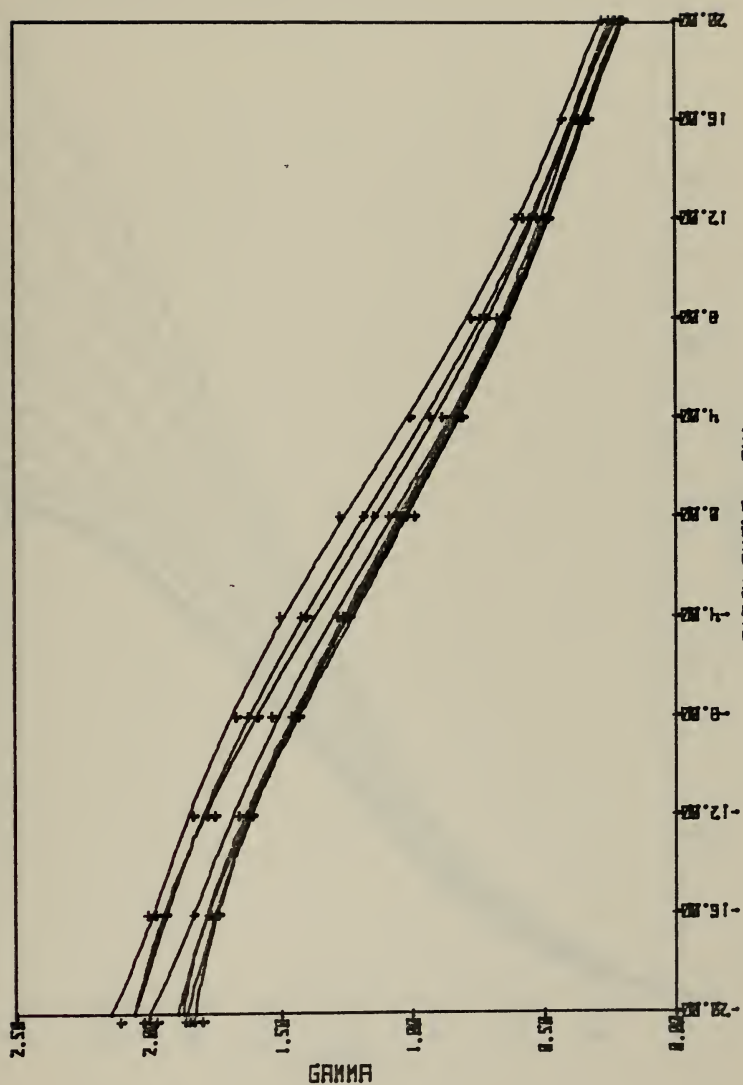


FIG. 19. GAMMA VS. PHI DATA POINTS AND POLYNOMIAL CURVE FITS.



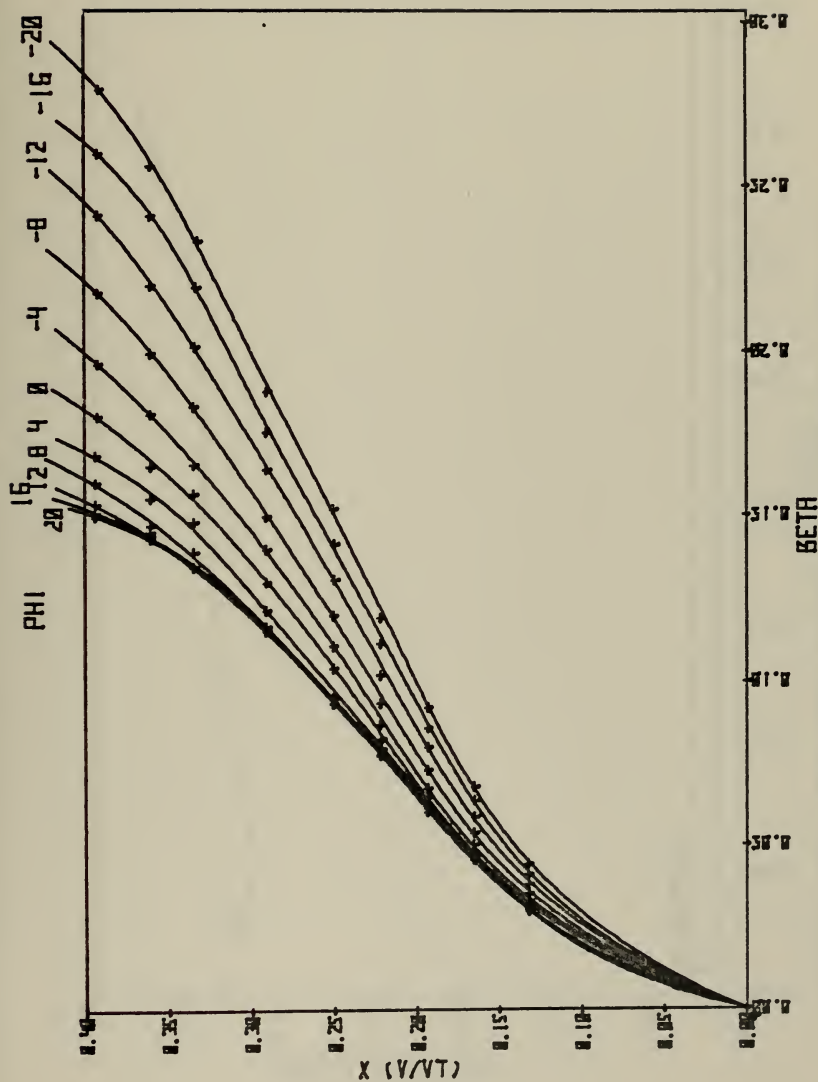


FIG. 20.  $X$  VS. BETA DATA POINTS AND POLYNOMIAL CURVE FITS.





FIG. 2.1. COEFF. FROM CURVE FIT ON FIG. VS. X.



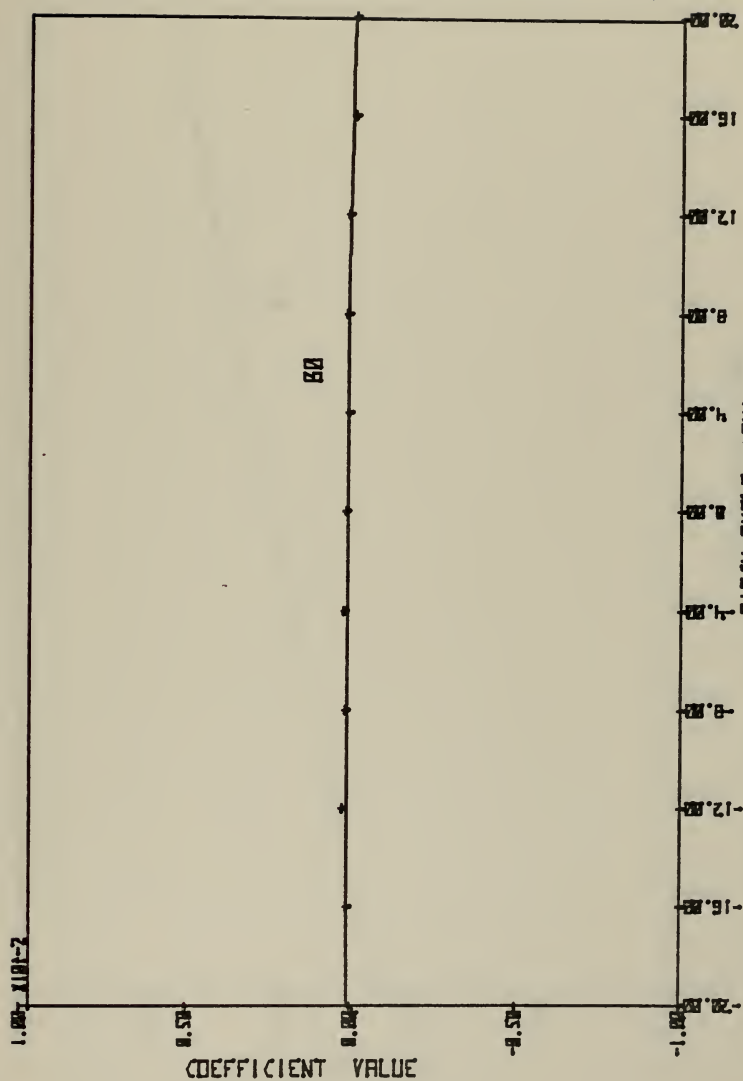


FIG. 22. CURVE FIT TO DETERMINE COEFF. FOR  $B_0$ .



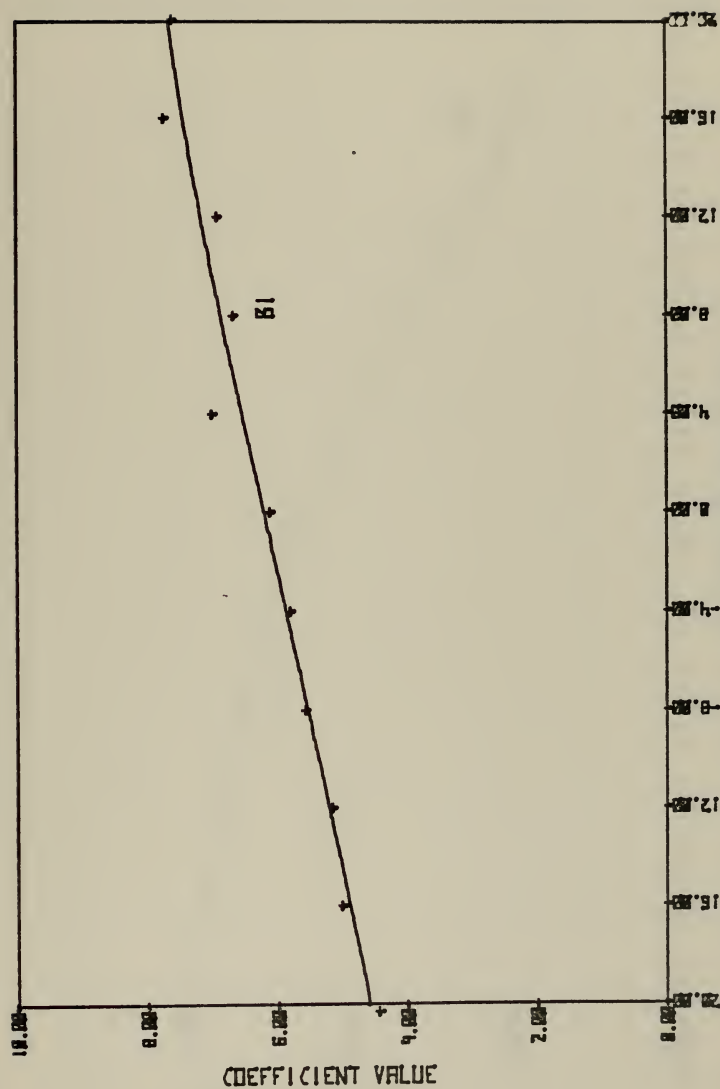


FIG. 2.3. POLYNOMIAL CURVE FIT TO DETERMINE COEFF. FOR B1.



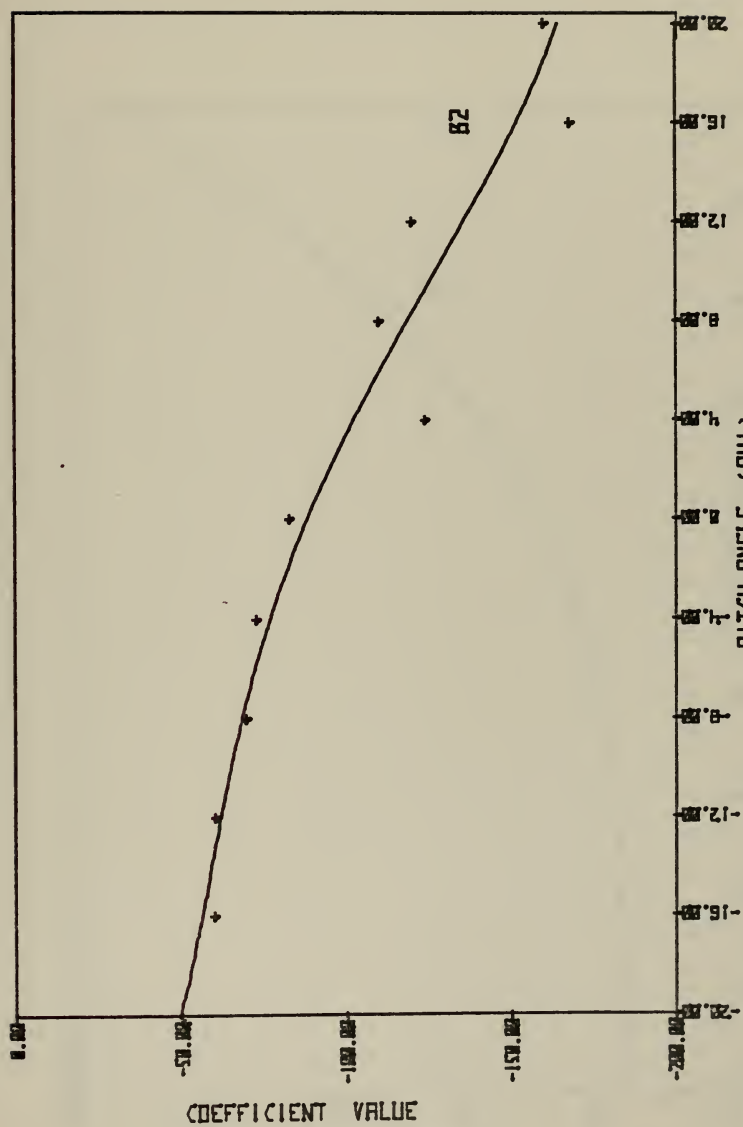


FIG. 24. POLYNOMIAL CURVE FIT TO DETERMINE COEFF. FOR B2.



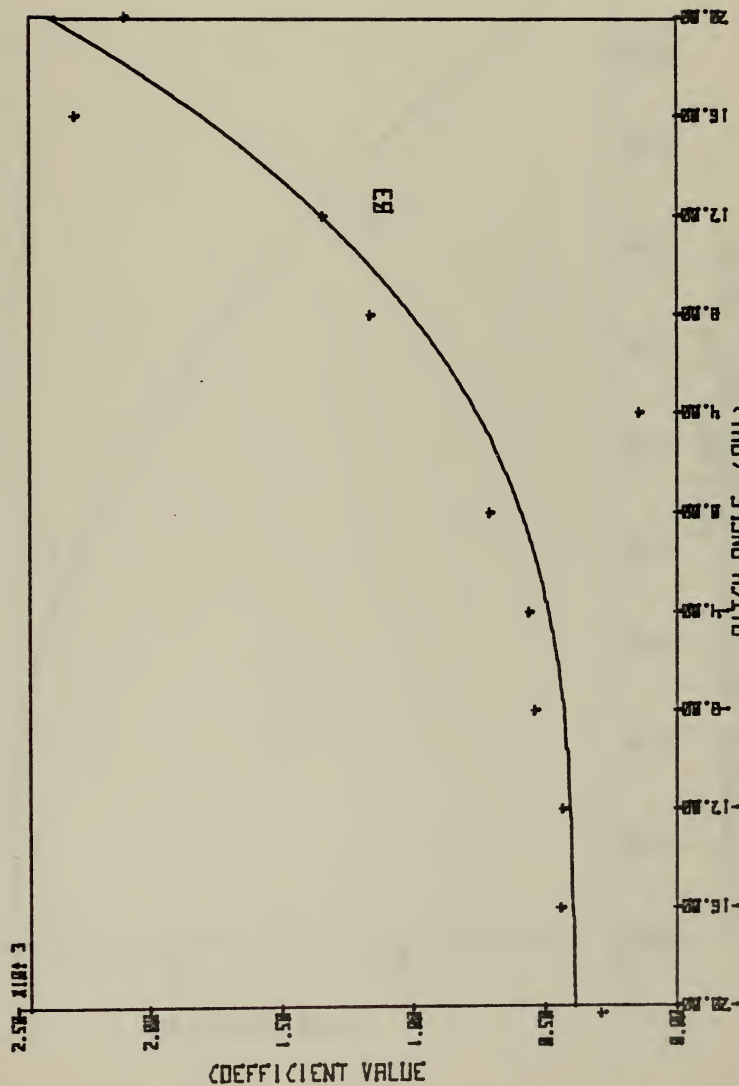


FIG. 25. POLYNOMIAL CURVE FIT TO DETERMINE COEFF. FOR B3.



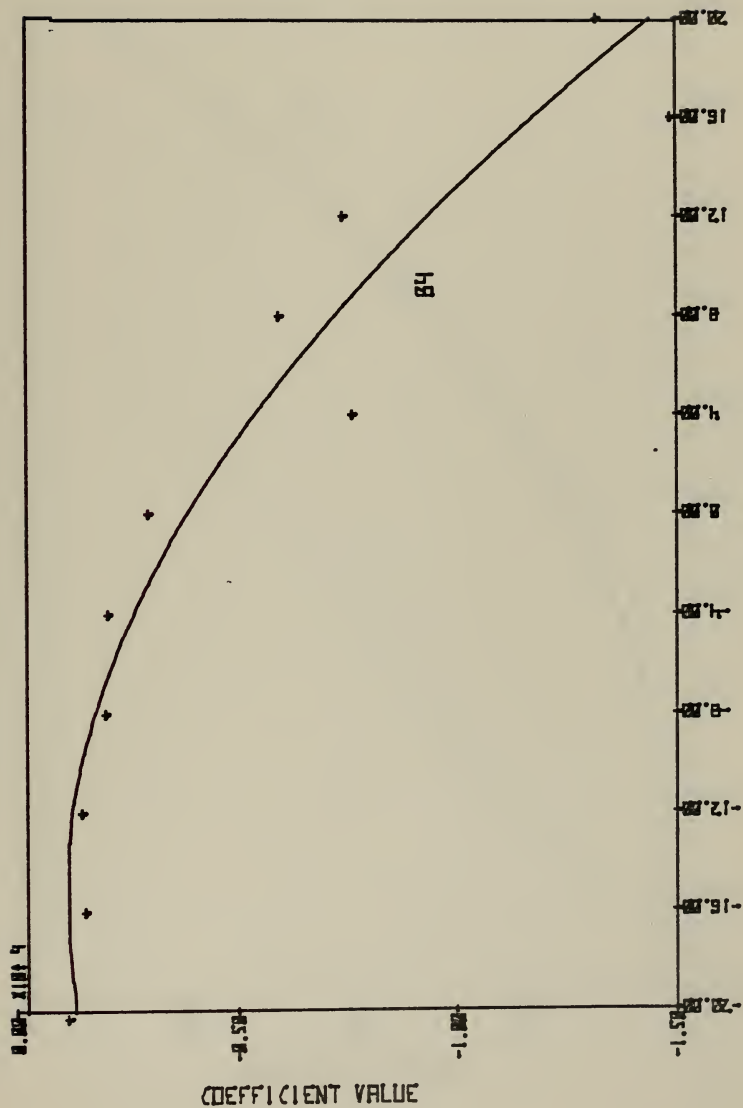


FIG. 2.6. POLYNOMIAL CURVE FIT TO DETERMINE COEFF. FOR 84.



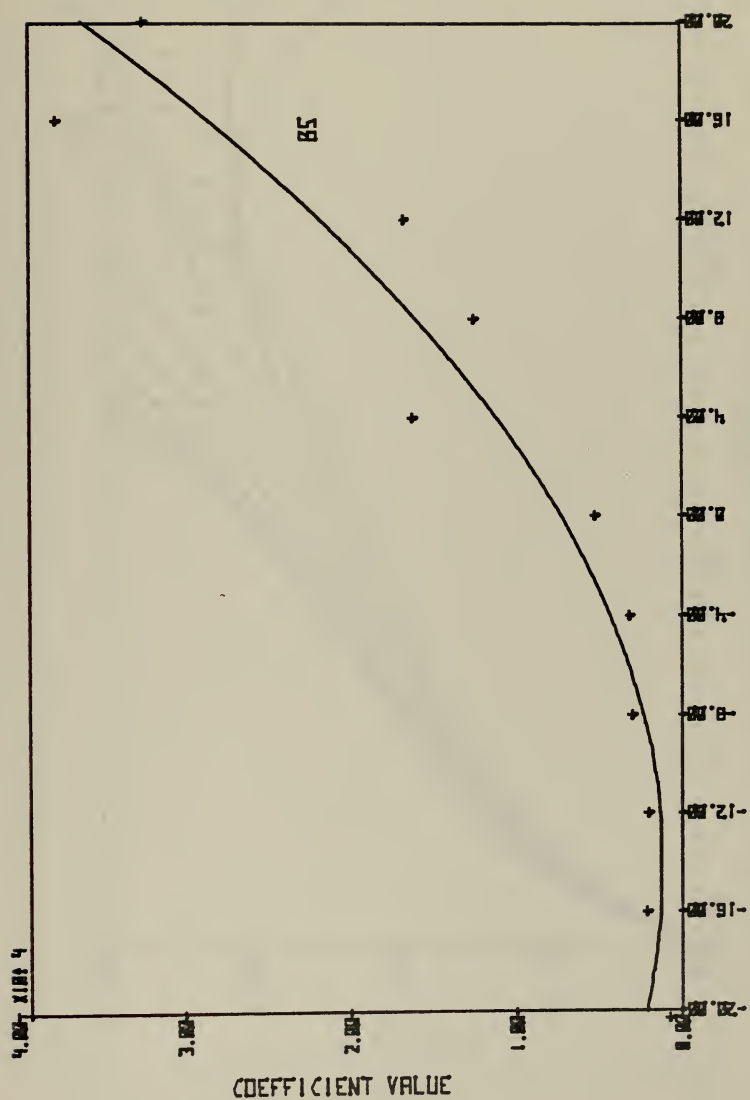


FIG. 27. POLYNOMIAL CURVE FIT TO DETERMINE COEFF. FOR BS.



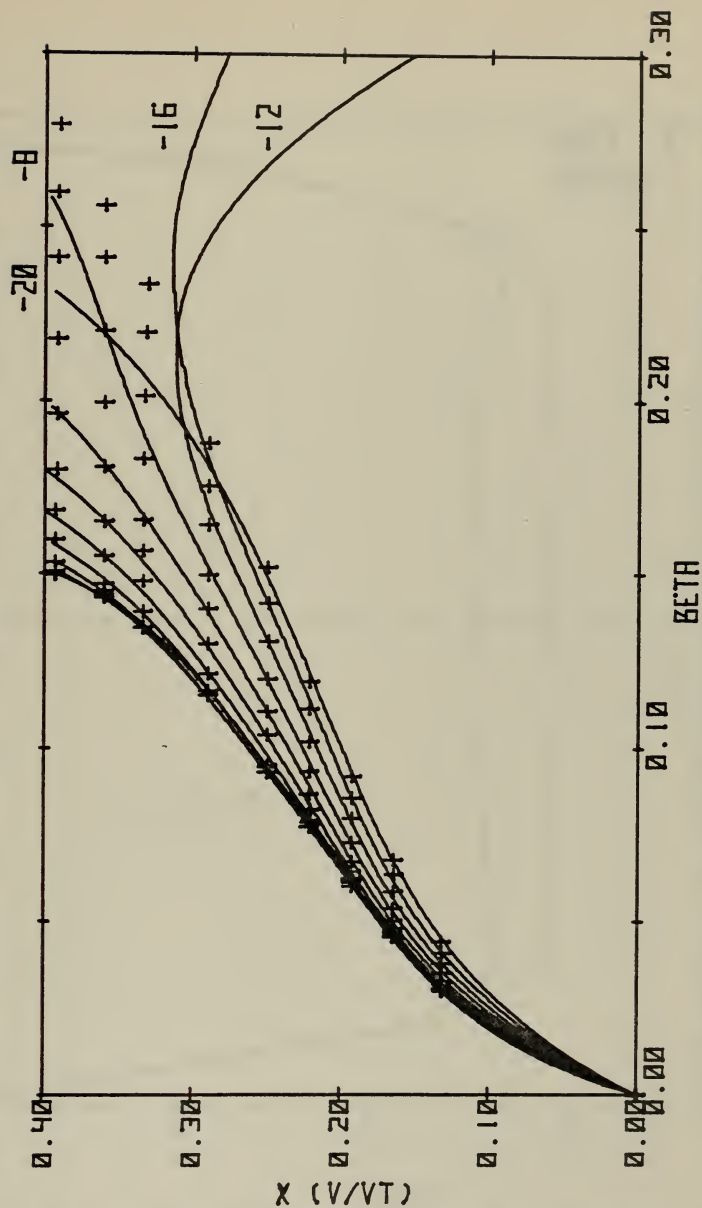


FIG. 28.  $X$  VS.  $BETA$  FOR EXPERIMENTAL DATA VS. PROGRAM POLYNOMIAL CURVE FIT.



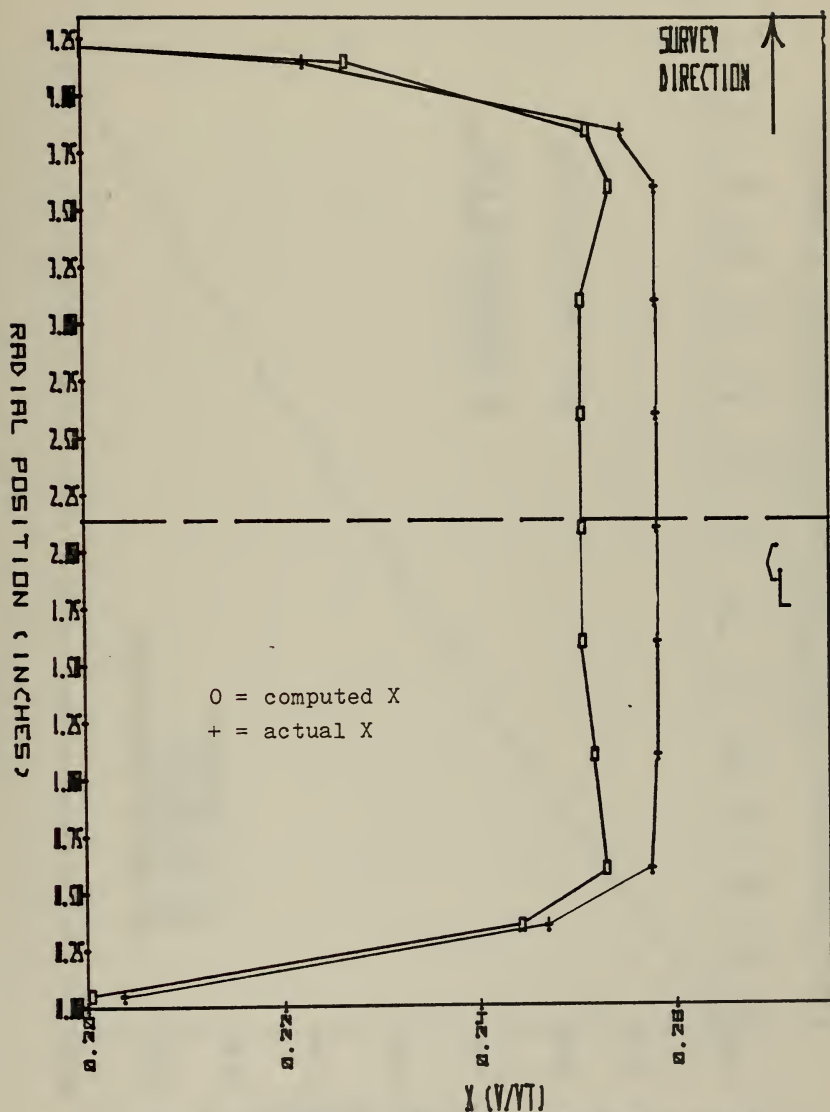


FIG. 29. VELOCITY PROFILES IN MEASUREMENT PLANE OF THE 4.2° NOZZLE.



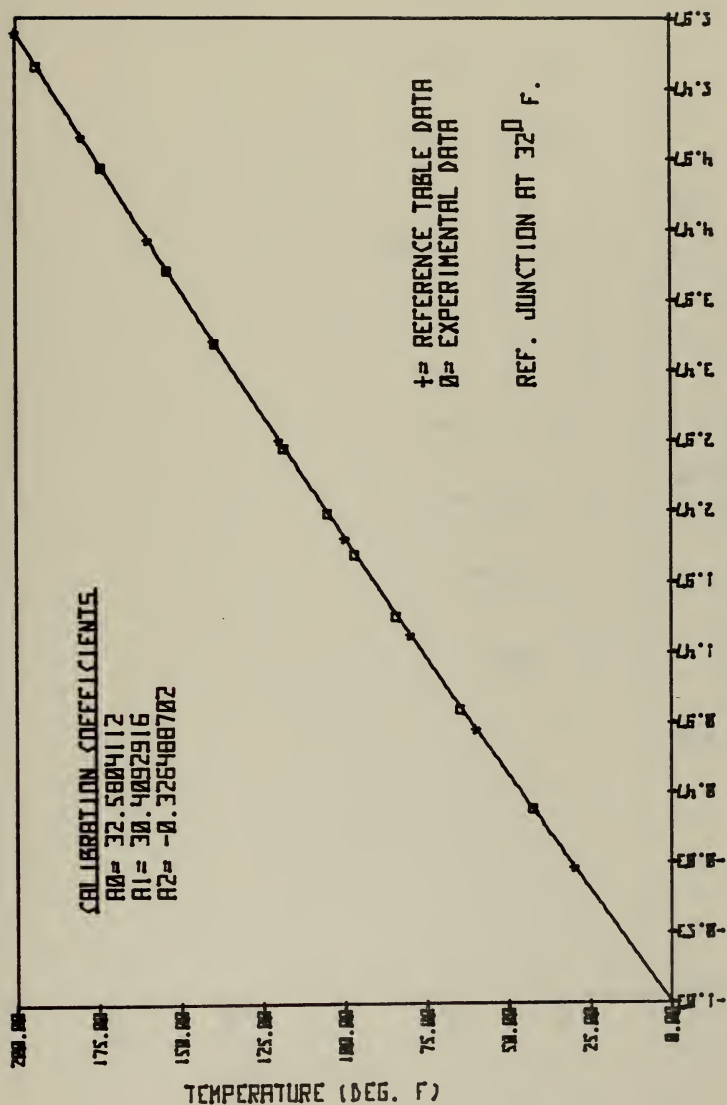
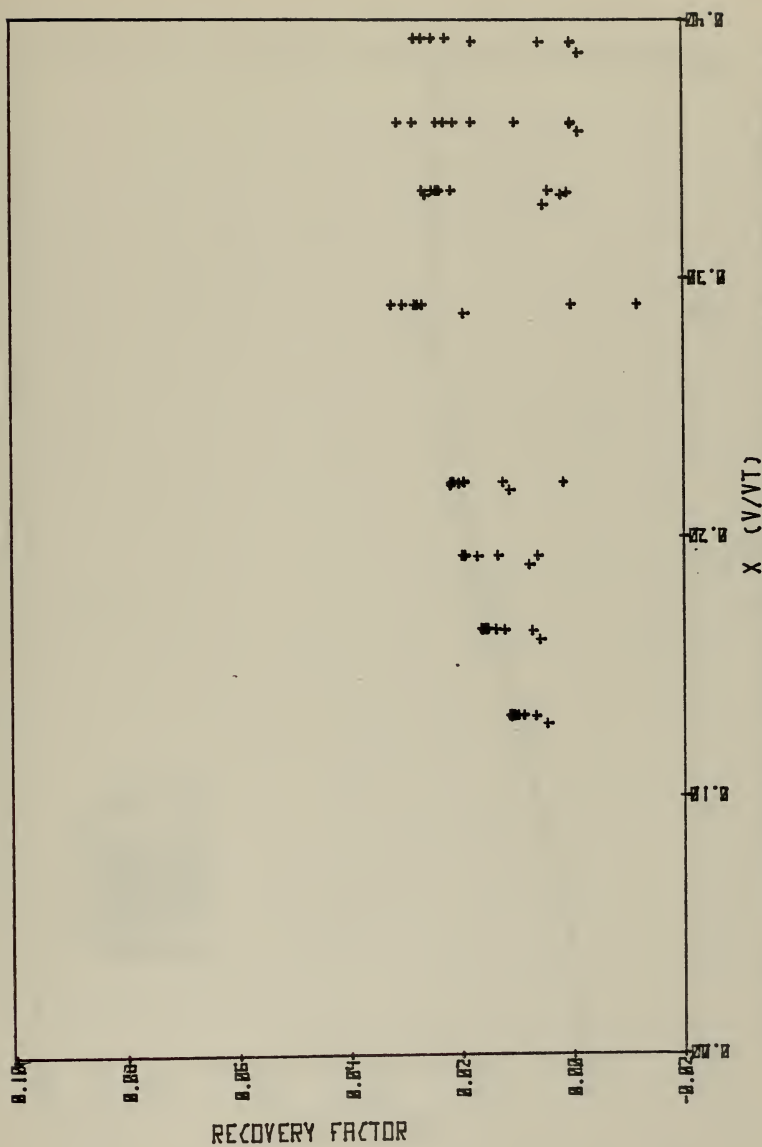


FIG. 30. EXPERIMENTAL DATA VS. REF. DATA FOR THERMOCOUPLE CALIBRATION.







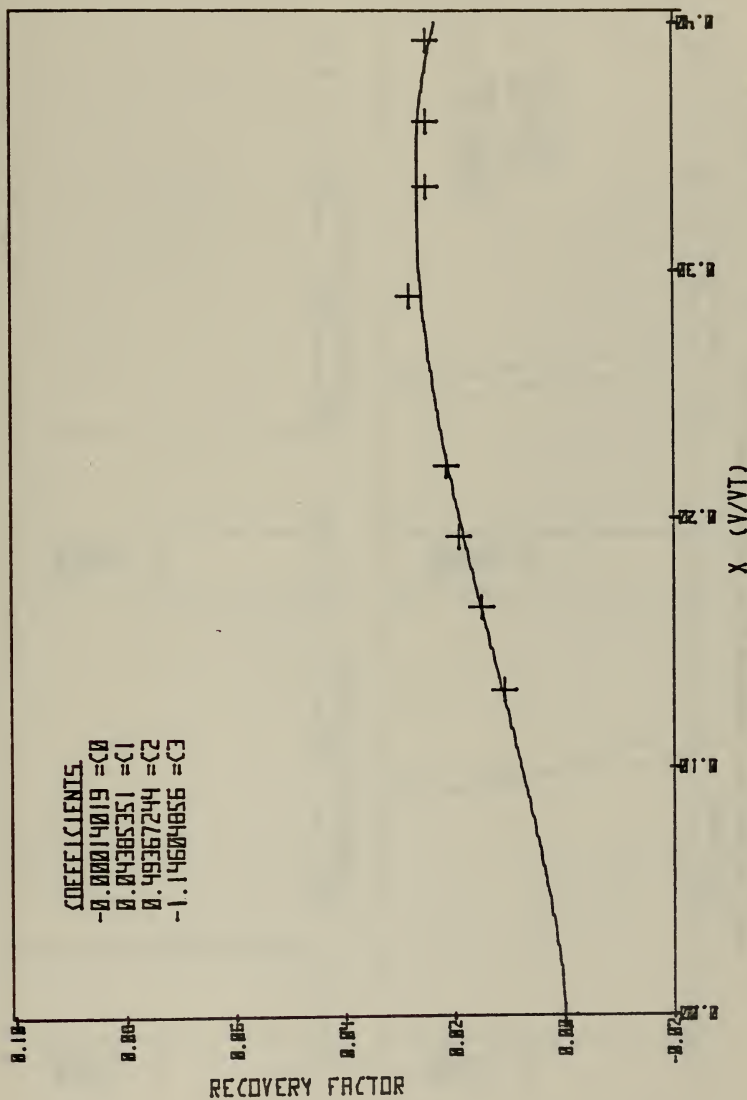


FIG. 32. DETERMINATION OF RECOVERY FACTOR COEFFICIENTS FOR TEMP. CALIBRATION.



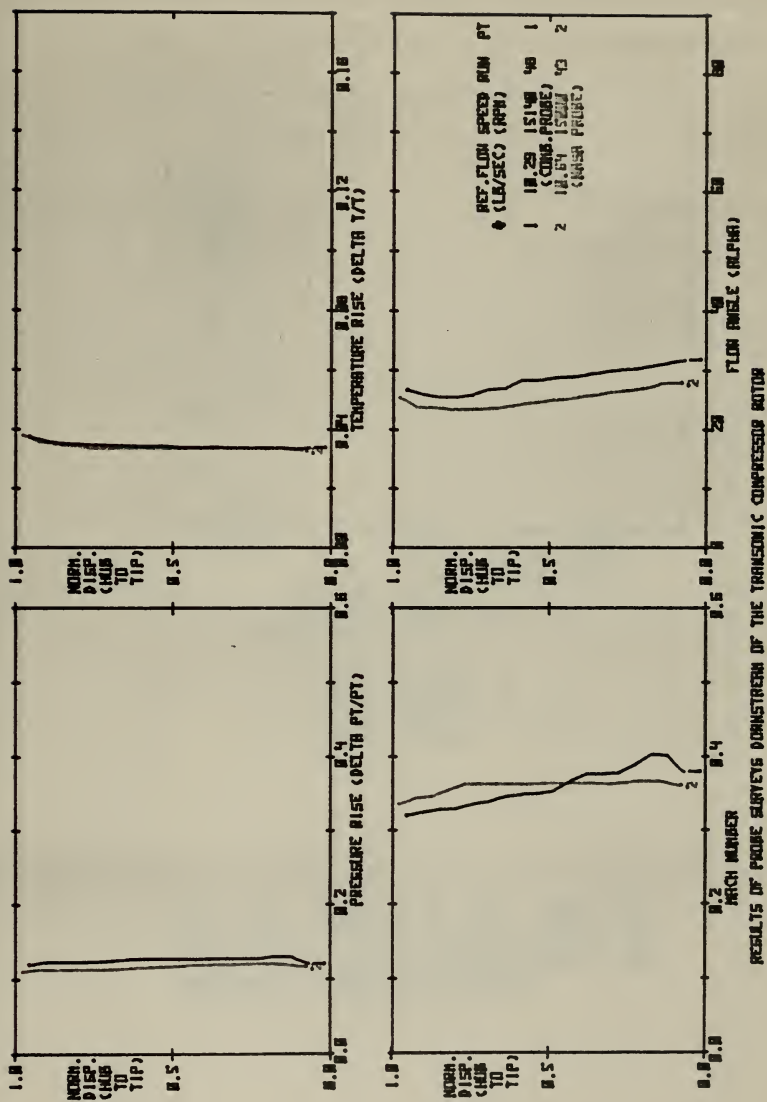
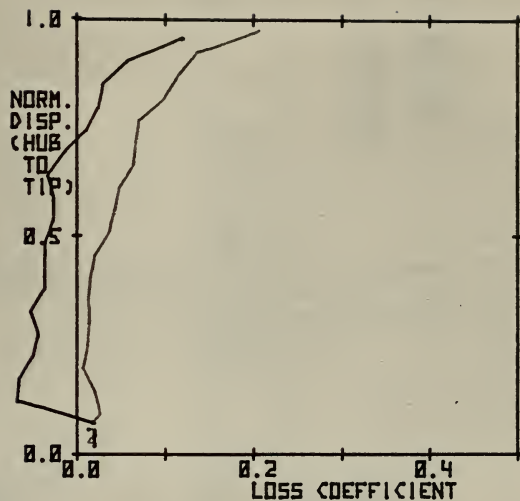


FIG. 33. RESULTS OF PROBE SURVEYS DOWNSTREAM OF TRANSONIC COMPRESSOR ROTOR.

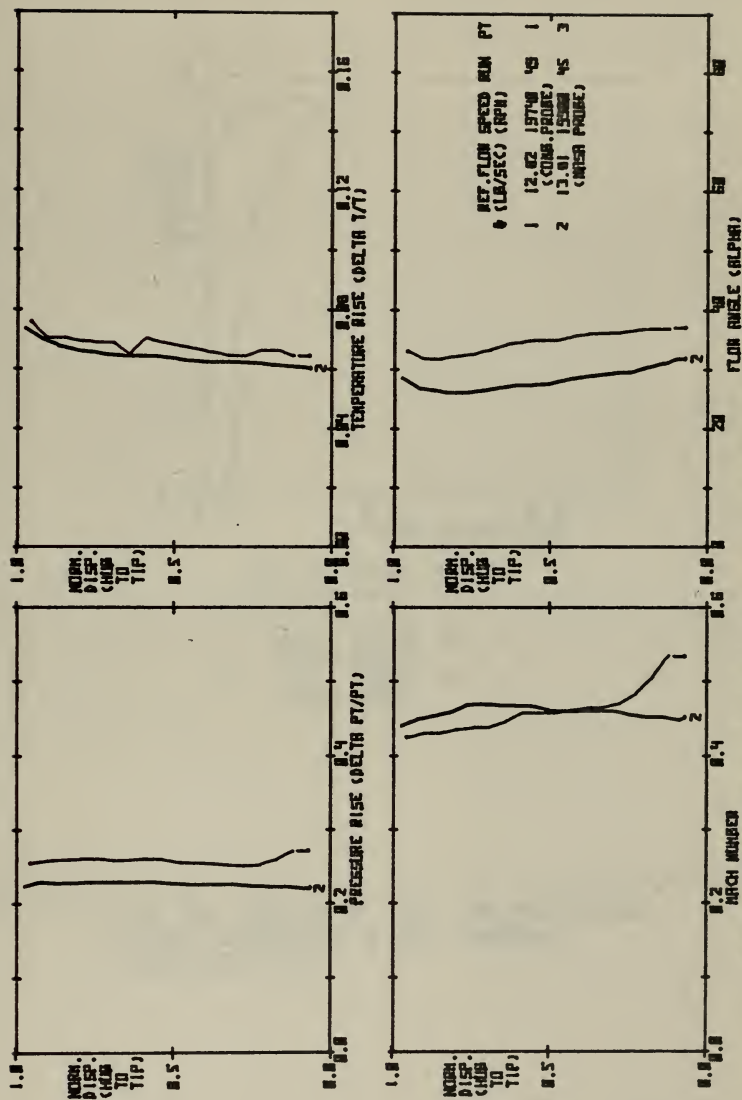




	REF. FLOW	SPEED	RUN	PT
#	(LB/SEC)	(RPM)		
1	10.29	15140	48	1
	(COMB. PROBE)			
2	10.64	15000	43	2
	(NASA PROBE)			

FIG. 34. RESULTS OF COMB. PROBE AND NASA PROBE SURVEYS DOWNSTREAM OF THE TRANSONIC COMPRESSOR ROTOR.

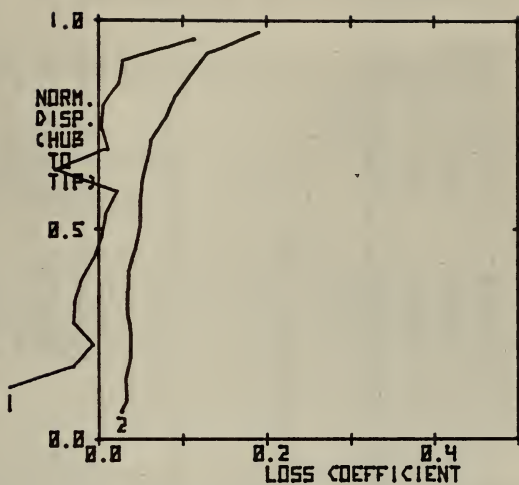




RESULTS OF PROBE SURVEYS DOWNSTREAM OF THE TRANSONIC COMPRESSOR ROTOR

FIG. 35 RESULTS OF PROBE SURVEYS DOWNSTREAM OF THE TRANSONIC COMPRESSOR ROTOR.





REF. FLOW SPEED RUN PT  
\* (LB/SEC) (RPM)

1	12.02	19740	49	1
				(COMB. PROBE)
2	13.01	19900	45	3
				(NASA PROBE)

FIG. 36. RESULTS OF COMB. AND NASA PROBE SURVEYS DOWNSTREAM OF THE TRANSONIC COMPRESSOR ROTOR.



TABLE 1. Coefficients for Eq. (11)

Order of Coeff.	$a_i(x)$	$a_i^1(x)$	$a_i^2(x)$	$a_i^3(x)$	$a_i^4(x)$	$a_i^5(x)$
Zereth	1.01900282	-0.0540280	3.1785E-04	-2.4054E-06	-3.5237E-08	2.6366E-09
First	0.37622122	0.0654377	-4.5788E-03	4.6765E-07	-2.0531E-06	1.2091E-07
Second	-3.98914949	-0.4144154	0.34764416	1.9038E-03	-1.4824E-05	-2.8915E-06
Third	11.65223670	0.5456268	-0.06911018	-3.9729E-03	5.8555E-05	5.64503E-06
Fourth	0	0	0	0	0	0
Fifth	0	0	0	0	0	0

TABLE 2. Coefficients for Eq. (12)

Order of Coeff.	$b_i(\phi)$	$b_i^1(\phi)$	$b_i^2(\phi)$	$b_i^3(\phi)$	$b_i^4(\phi)$	$b_i^5(\phi)$
Zereth	7.7033E-05	6.2493119	-90.5810935	841.42914	-3886.00047	7310.0931
First	-2.8275E-06	8.653E-02	-3.17818846	50.989039	-341.952955	849.98435
Second	-1.8496E-07	-2.732E-04	-4.5213E-02	1.1448488	-9.97539102	29.361298
Third	4.1464E-11	-2.559E-05	8.1759E-04	-1.117E-02	0.03872750	-3.380E-03
Fourth	0	0	0	0	0	0
Fifth	0	0	0	0	0	0

The 4th and 5th order coefficients are shown because the reduction routine was developed for a fifth order polynomial expression.



TABLE 3. Error Analysis of Limiting Velocity Computation

$\phi$	X1	X	$\phi/E$	X1	X	$\phi/E$	X1	X	$\phi/E$
-4	.131396	.129285	1.60	.164710	.165297	0.35	.192627	.191730	0.46
0	.131396	.130828	0.43	.164718	.165110	-0.24	.192935	.192594	0.21
4	.131396	.129404	1.51	.164718	.166898	-1.32	.192935	.192118	0.42
8	.131396	.130242	0.88	.164718	.165229	-0.35	.192781	.191543	0.64
12	.131396	.131874	-0.36	.164718	.165996	-0.77	.192871	.193840	-0.55
16	.131644	.133040	-1.00	.164718	.165610	-0.54	.192781	.193306	-0.27
20	.131396	.132291	-0.68	.164718	.164603	-0.07	.193089	.191566	0.79
	①								
-4	.221760	.218644	1.40	.290028	.294044	-1.38	.360171	.355704	1.24
0	.220744	.219991	0.34	.290028	.291638	-0.55	.360171	.358448	0.48
4	.221380	.220357	0.29	.290028	.290876	-0.29	.360171	.362492	-0.64
8	.221380	.220799	0.26	.290028	.288612	0.48	.360171	.355278	1.35
12	.221506	.221904	-0.18	.290028	.291148	-0.38	.360171	.354340	1.61
16	.221125	.223357	-1.00	.290028	.291594	-0.53	.360171	.364102	-1.09
20	.220744	.221854	-0.50	.290028	.286894	1.08	.360171	.366700	-1.80
	②								
-4	.355704	.355704	0.00	.360171	.360171	0.00	.360171	.360171	0.00
0	.358448	.358448	0.00	.362492	.362492	0.00	.362492	.362492	0.00
4	.355278	.355278	0.00	.355278	.355278	0.00	.355278	.355278	0.00
8	.354340	.354340	0.00	.354340	.354340	0.00	.354340	.354340	0.00
12	.364102	.364102	0.00	.364102	.364102	0.00	.364102	.364102	0.00
16	.366700	.366700	0.00	.366700	.366700	0.00	.366700	.366700	0.00
20	.366700	.366700	0.00	.366700	.366700	0.00	.366700	.366700	0.00
	③								

$\phi$  = pitch angle  
 X = actual value  
 X1 = computed value  
 $\phi/E$  = percent error

Data Set      Mach No.

- ① . 0.295  
 ② 0.372  
 ③ 0.437  
 ④ 0.506  
 ⑤ 0.675  
 ⑥ 0.861



TABLE 4. Results of applying polynomial reduction program data taken from a separate traverse of the flow through the 4.2 inch nozzle (see Fig. 29)

DODGE Probe Survey #3			
R/R0	X(actual)	X(computed)	%Error
0.0238	0.204271	0.201019	1.59
0.0833	0.246958	0.244270	1.08
0.1428	0.257555	0.252873	1.82
0.2619	0.258226	0.251700	2.52
0.3809	0.258226	0.250592	2.96
0.5000	0.258226	0.250592	2.96
0.6190	0.258226	0.250592	2.96
0.7381	0.258226	0.250592	2.96
0.8571	0.258226	0.253599	1.79
0.9166	0.254748	0.251229	1.38
0.9880	0.222470	0.226722	-1.02



## APPENDIX A

### Fabrication of the Thermocouple Sensor

#### A.1 Introduction

Much knowledge and experience was gained from the development and application of the combination probe. In particular, the refinement of a fabrication procedure which would allow for the duplication of the thermocouple sensor installed in the combination probe is most important. It is the purpose of this Appendix to outline a time-tested procedure, using a limited number of tools, that will permit the fabrication of a nearly identical thermocouple sensor to that installed in the combination probe. The following sections outline a step-by-step procedure for the preparation and wiring of the insulator to meet this objective.

A few important words of wisdom might be interjected at this point before construction of a thermocouple is commenced. One may initially believe that with a good eye and a steady hand, success is assured. These are commendable assets but success can be attained without them. Extremely high levels of concentration can develop at certain points in the fabrication process. The following suggestions may appear trivial but they are far and away the most important ingredients to the successful development of a small fine wire thermocouple sensor.



First and most importantly, find a quiet undisturbed location with no distractions and good lighting to do the work. Even small drafts in a room can significantly compound the problem of feeding fine wires into the insulator.

Secondly, relax. Do not attempt to work if it is felt that rushing to get the job done is necessary. It will only result in frustration and a considerable waste of time.

Finally, maintain a positive attitude. Certain parts of this procedure are difficult, particularly when attempted for the first time. Do not continue on with a technique if it does not work the first few times that it is attempted. It is a fact that all the mistakes that could have been made in the fabrication of this sensor have been made. It is unnecessary to spend considerable time proving that they can be made again.

## A.2 Equipment and Materials

Sophisticated equipment will no doubt enhance the quality of the product. The fabrication of the fine wire thermocouple in this report was completed with tools that are readily available in most workshops and laboratories. The possible exceptions might be the first two pieces of equipment listed below.

### A.2.1 Equipment

1. High speed, 30 mil thick diamond cutting wheel. This device cuts the notch in the



insulator that will ultimately seat the thermocouple.

2. Spotwelder. A 1065 Unitek 20-100 watt/sec spotwelder was used to weld the 1 mil to the 2 and 5 mil wires.
3. 4.0X power magnifying device. This is an invaluable aid which is used at nearly every stage in the fabrication process.
4. Tweezers (2 pair). A pointed pair is necessary to work in small areas and a cosmetic pair is suitable for gripping and pulling wires.
5. Scissors.
6. Needles. Sewing needles work perfectly for centering and bending wires; applying coatings.
7. Hot air blowing device. This is used to heat the "shrink-fit" material that supports the 5-mil wiring on the internal probe shaft arrangement.

#### A.2.2 Materials

1. 32 mil mullite, 2-hole insulator.
2. 1 mil chromel-constantan thermcouple and wire.
3. 2 mil stiff bare wire (chromel was available).
4. 5 mil insulated chromel and constantan wire.
5. 1/16 to 1/4 inch O.D. shrink-fit material.
6. Nonconductive, pliable cement (G-S Hypo-Tube cement; Germanon-Simon Machine Co. was used).



7. Liquid insulator (Urathane Seal Coat Electric insulator by CRC Chemicals was used).

### A.3 Fabrication of Insulator Notch

The following procedure outlines a method to machine the insulator to accomodate a small notch that is 30-35 mils in length on one side of the insulator (Fig. A.1).

1. Insert a selected insulator into the housing tube on the combination probe to insure that it fits. Tolerance limits on the outer diameter of Omega mullite insulators were a problem.
2. Make a small plastic jig (Fig. A.2) to firmly support the insulator while the notch is being made.
3. Support the jig (with insulator) on the diamond cutting apparatus. It is desired to make the notch as near the end of the insulator as possible, although it was found that the end of the insulator would break if at least a 50 mil space did not exist between the notch and the end of the insulator (Fig. A.2).
4. The notch should be made until both holes in the insulator are exposed. Do not remove more than a  $\frac{1}{2}$  mil thickness per cut in the insulator since the chances of its breaking increase rapidly as the notch depth increases and the amount removed increases.



5. The product should look like the notched insulator shown in Fig. A.1. Mr. Glenn Middleton, in the Department of Aeronautics at the Naval Postgraduate School, is familiar with this procedure.

#### A.4 Fabrication of the Sensor

1. Insert the notched insulator back into the housing tube on the probe and locate it exactly where it will be in the final installation.
2. Mark the insulator with a felt-tip pen about  $\frac{1}{4}$  inch outside the threaded part of the probe shaft (Fig. A.3(a)). Remove the insulator and center the mark between the thumb and forefinger of each hand. A firm but gentle snap will break the insulator to the desired length (Fig. A.3(b)).
3. Stretch a 6-8 inch length of 2 mil (chromel) wire and cut off the turned or twisted ends so that a straight piece of wire at least 5 inches long remains.
4. Take the wire between the thumb and forefinger and gently, steadily feed the wire into one of the holes in the insulator (Fig. A.4). Do not use tweezers to feed the wire since kinks will occur making the wire impossible to feed through the length of the insulator. If a kink occurs, begin again at step 3.



5. When the wire is fed through the entire length of the insulator, twist the end of the wire at the notched end of the insulator as shown in Fig. A.5(a). The pointed tweezers work well here.
6. Pull the wire back through the insulator until the end of the wire just disappears inside the end of the insulator. Then support the insulator under the magnifying device. While viewing the notched section under the magnifier, pull the wire gently until the end of the wire appears in the notch. If the end of the wire does not immediately pop up out of the hole, then take tweezers and gently move the wire back and forth in the notch until it pops up. If the wire still does not pop up or is pulled too far past the notch, then remove the wire and begin again at step 3.
7. When the end of the wire has popped up in the notch (Fig. A.5(b)), use a sewing needle to bend the wire so that it sticks straight up out of the notch (Fig. A.5(c)). Pointed tweezers may then be used to pull the wire out of the hole about 1.5 inches. With scissors, cut off the end of the wire that was twisted leaving about 1 inch of straight wire protruding from the notch.
8. Repeat steps 3-7 for the second wire.
9. Wrap the thermocouple wire around the protruding 2 mil wire as shown in Fig. A.6(a). Spotweld the



two wires together. Unwrap the free end of the 1 mil thermocouple wire from the 2 mil wire to the first weld. With tweezers bend the 1 mil wire back and forth until it breaks at the weld (Fig. A.6(b)). This will eliminate the possibility of having to force a loose end of wire through the notch.

10. Support the notched section under the magnifier. Then, feed the welded section back through the notch using a needle to guide the initial weld into the hole. Once the initial part of the welded section has passed by the notched area, the remainder of the double-wired section should then easily pull through the insulator.
11. When the lead end of the thermocouple wire has been pulled completely through the insulator, tag the wire with a piece of tape to identify the wire as positive or negative.
12. Repeat steps 9-11 for the second wire.
13. With the insulator supported under the magnifying device, gently pull on each thermocouple wire until the thermocouple is properly seated in the center of the notch (Fig. A.1). Once seated, tug the two thermocouple wires gently (in unison) to form the thermocouple head and wire to the notch geometry. Then, after insuring that the wires are not crossed at the end of the insulator, apply a small dab of



nonconductive cement to the holes as shown in Fig. A.7 to hold the thermocouple in place.

14. Cut two pieces of 5 mil insulated wire, one chromel and the other constantan. Bare about one inch of the end of each wire. Then, using the same procedure outlined in Step 9, wrap the 1 mil thermocouple wire around the 5 mil wire and spotweld in several places. Do not attempt to wrap the 5 mil wire so that it makes contact with the end of the insulator. Leave a space about  $1/8 - 1/4$  inch as shown in Fig. A.8.
15. After the spotwelding is completed, remove any excess thermocouple wire by the bending procedure suggested in Step 9.
16. Apply several coats of liquid insulator to these bare wire sections. After allowing the freshly insulated sections to dry, the sensor may be installed in the probe.
17. When the insulator is properly located in the thermocouple sensor housing tube, apply cement to the insulator at the point where it exits the tube. This is near the threaded junction (Fig. A.3(a)).
18. Use the shrink-fit material to hold the 5 mil wires and pressure tubes together along the length of the internal shaft. Be careful not to overheat the section of wiring where the liquid insulator has been applied.



19. Attachment of the outer shaft assembly of the probe and wiring the connector will complete the thermocouple sensor fabrication. The combination probe will be ready for use after 24-48 hours of drying time.

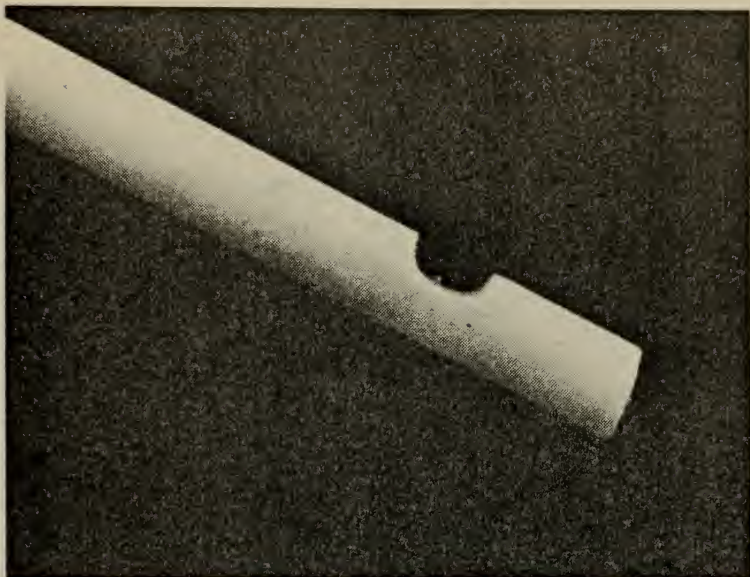
A.4.1 Spotwelding

The Unitek spotwelder that was used for this work had no calibrated pressure setting; only an adjustable screw was installed. The power output of the instrument was set at 1.2 watts/sec for most of the welds and the pressure screw was adjusted by trial and error until a good weld was obtained without breaking the 1 mil wire. Peecher, in Ref. 7 recommended the following welder settings if a pressure adjustment (calibrated) was installed:

pressure = .2

power = 1.2 watts/sec





Side view

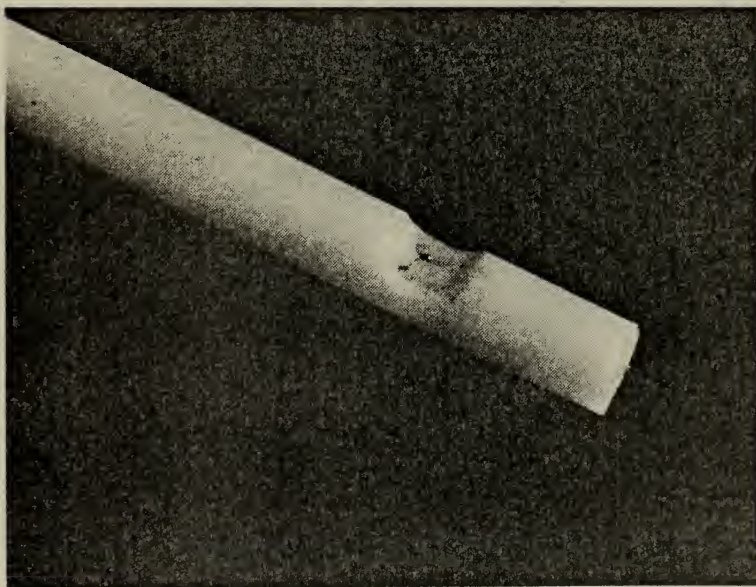


FIG. A1. Photographs of insulator notch



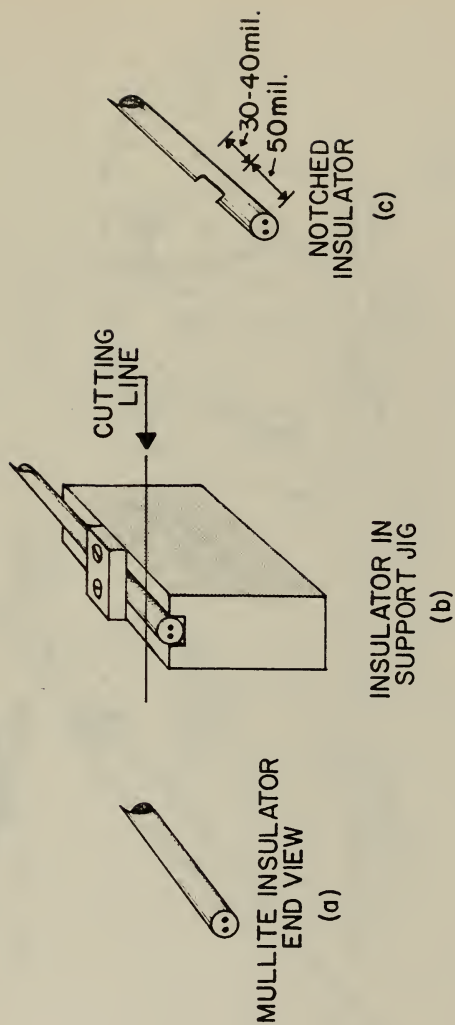


FIGURE A2



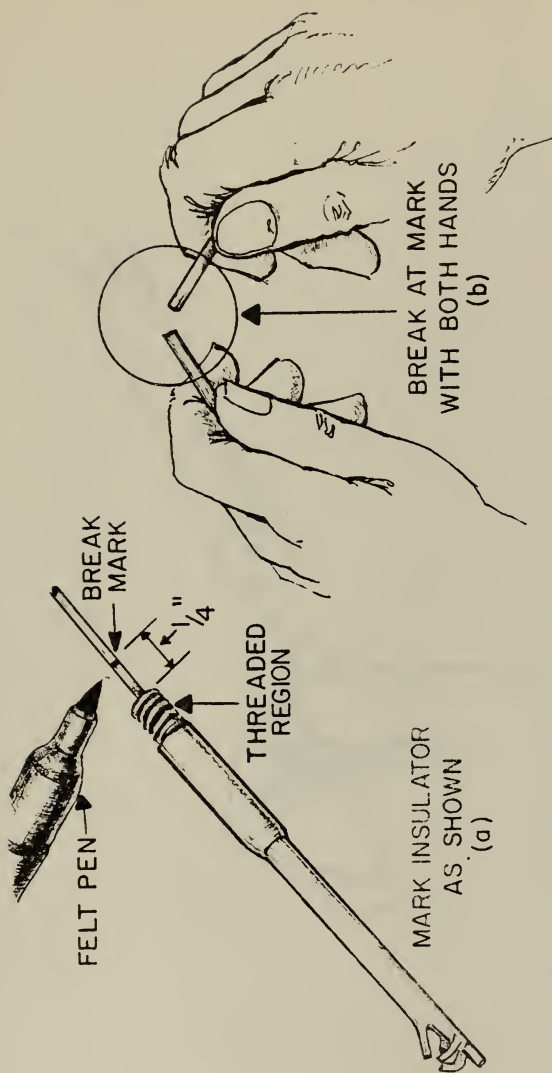


FIGURE A3



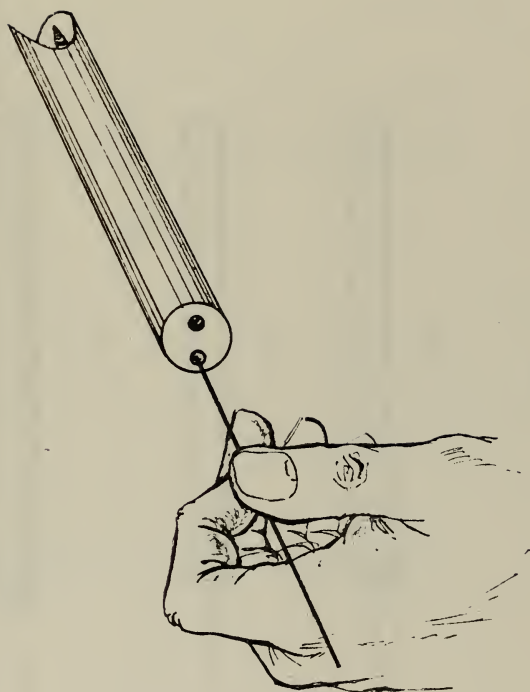


FIGURE A4



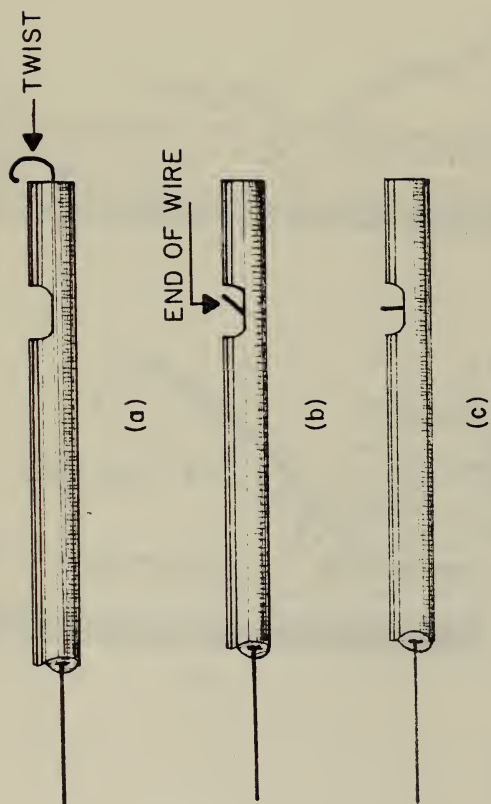


FIGURE A5



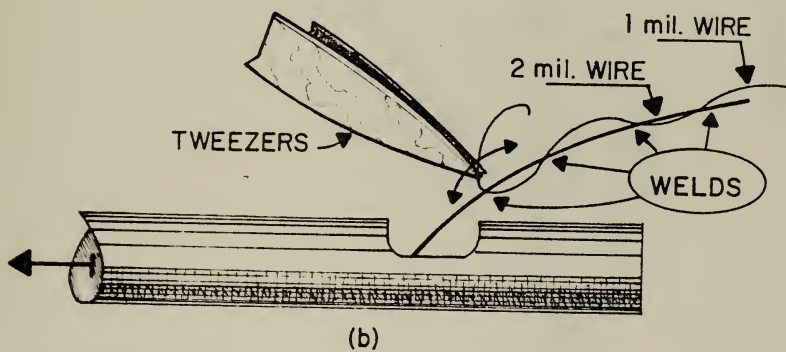
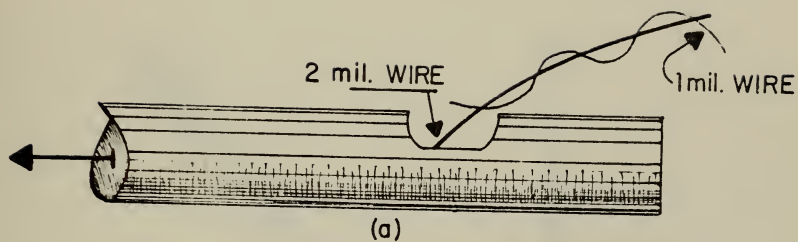


FIGURE A6



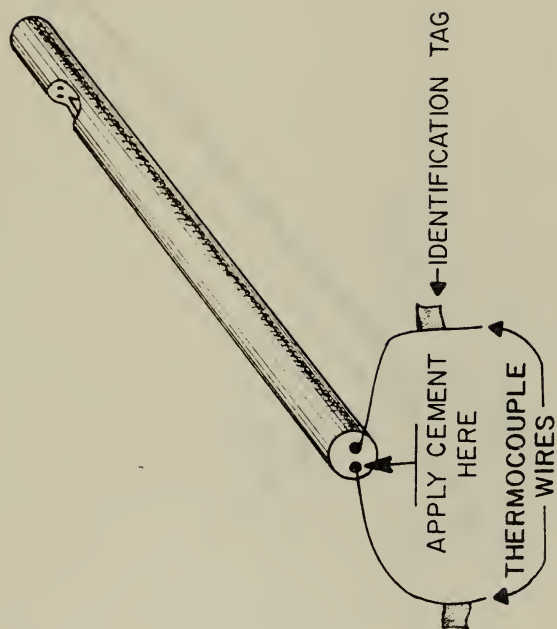


FIGURE A7



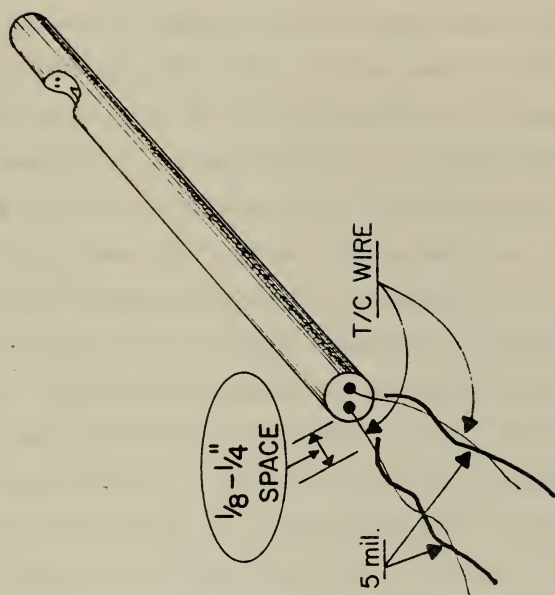


FIGURE A8



## APPENDIX B

### Improvements to the Probe Calibration Apparatus

#### B.1 Introduction

A desirable goal is to develop a general calibration procedure whereby a complete set of calibration curves may be obtained for any probe that will be used for flow measurements. The first step in the calibration of a probe is to obtain a measure of its performance in a known uniform flow. The free jet apparatus at the Turbopropulsion Laboratory provides such a flow. The apparatus, which is fed by a high pressure air supply, consists of a plenum and a ten inch supply pipe to which a nozzle is attached (Fig. B.1). Flow straighteners are installed in the pipe to ensure that the flow is everywhere axial. Currently, there are two nozzles (7 inch and 4.2 inch) available to provide flow velocities that range from zero to supersonic speeds. Only the 4.2 inch nozzle can be choked since the air supply is limited to about 11 lbs. per sec. at 3 atmospheres pressure.

The application of the probes is generally to determine the flow in an annulus. A straight annulus has been designed to match in size the annulus in the transonic compressor. In this apparatus the wall effects can be measured in conjunction with stem and interference effects that are introduced when the probe is immersed in a



contained flow. From these measurements corrections to the free-flow calibration of the probe can be derived, which can be applied to transonic compressor flow field measurements. Figure B.2 shows the straight annulus at the Turbopropulsion Laboratory.

In order to more nearly duplicate the type of flow in the transonic compressor, a swirl annulus was recently developed. Turning vanes were installed in the entrance to the annulus to turn the flow from axial to provide a controlled swirling flow representative of the flow conditions in the transonic compressor. The swirl annulus is shown in Fig. B.3.

Changes and improvements that have been made to the free jet and swirl annulus are described in the following sections.

## B.2 Probe Mounting Box

For the calibration of the pneumatic five-hole probe which was reported in Ref. 3 the probe was inserted through the wall of a ten inch pipe that contained a free jet. Calibration by this method introduced a small error, and no correction was made for static pressure varying across the flow. The development of a probe mounting box overcame this problem by allowing a probe to be mounted in a fully free jet at a point where the static pressure was truly atmospheric. This eliminated the requirement for a Prandtl probe measurement of static pressure.

The mounting box was constructed of available aluminum stock material. The box can be directly attached downstream



of either the 4.2 or the 7 inch diameter nozzle, with an adapter plate. Provisions have been made which allow for a traverse unit and/or a pitch angle survey mount to be directly attached to the mounting box. A splitter plate may also be supported by the box and aligned with the center of the flow for probe-boundary interference studies. Probes may be mounted on each side of the mounting box. Measurements can be made at the nozzle exit, or inside the nozzle if the probe has an extended tip. Figure B.4 shows front and side views of the mounting box attached to the ten inch pipe with the seven inch nozzle installed.

### B.3 Pitch Angle Survey Mount

The object of the data reduction from surveys in the transonic compressor is to reduce the probe measurements to values of Mach number and pitch angle. For this purpose, calibration tests must be carried out in which the Mach number and pitch angle are known and can be varied over a sufficient range.

Figure B.5 shows the side view of a pitch angle survey mount which was developed to provide a means for obtaining probe data as a function of pitch angle. In this device, the probe can be set in the free jet to any angle up to  $\pm 40$  degrees pitch. Measurements may be taken to within 1.1 diameters of the nozzle exit for a 4.2 inch nozzle and 0.75 diameters for a 7 inch nozzle. The device is mounted on the probe mounting box described above.



#### B.4 Honeycomb Section for the Swirl Annulus

The swirl annulus apparatus is shown in Fig. B.3. The device was designed to generate a controlled swirl in an annulus which could be used to examine the calibration of a probe in an environment similar to that found in the transonic compressor. Ideally, the flow field generated would have smooth radial variations in flow angle and velocity.

Initial testing of the apparatus revealed that 60 degree turning angles were produced by the vanes near the outer wall, but that there was a reversal of the flow at the hub. It was reasoned that the flow should exit axially to the uniform room pressure and consequently an adjustable honeycomb section was constructed from available materials. The honeycomb section was installed inside the swirl annulus shown in Fig. B.3. Further testing of this section is required in order to obtain the desired test conditions.



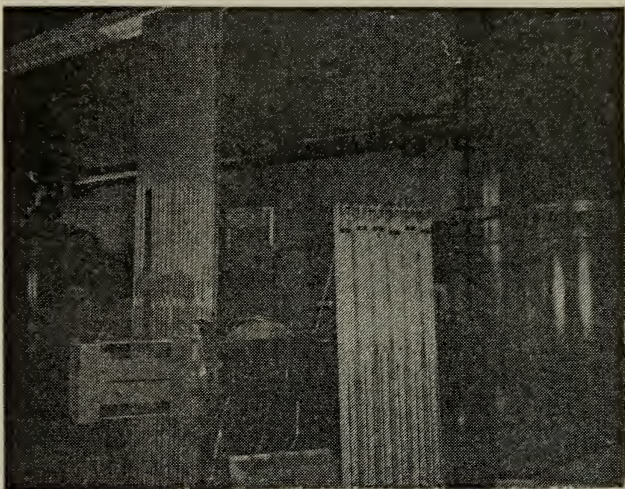


FIG. B1. Free jet apparatus.

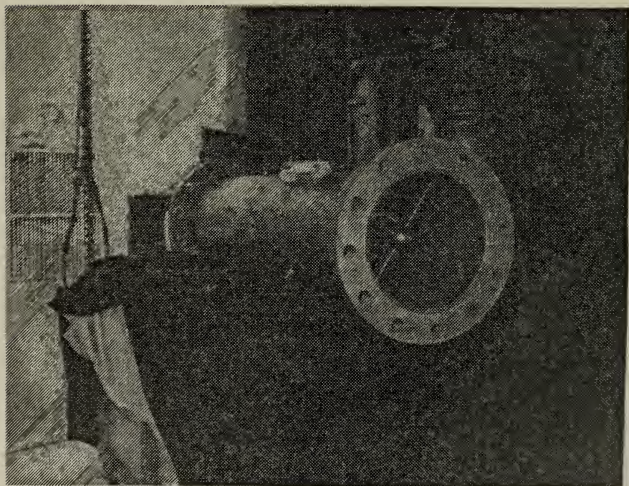
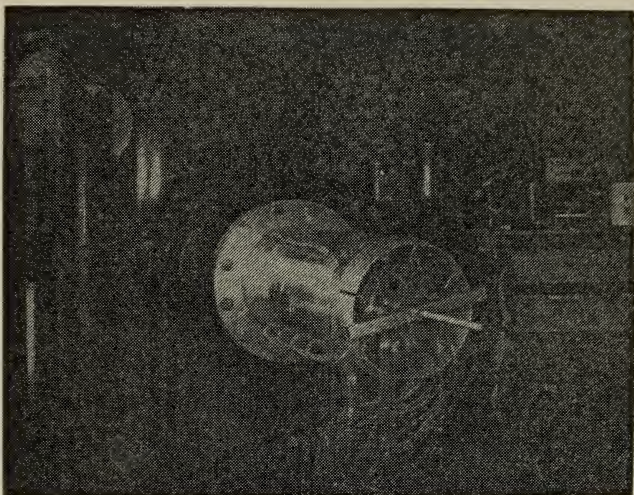
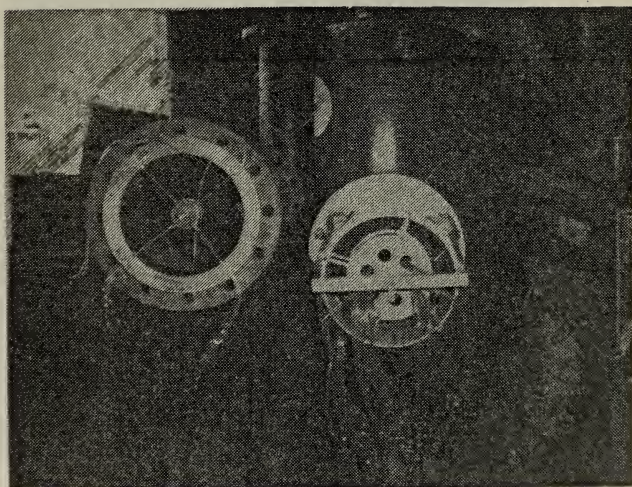


FIG. B2. Straight annulus.



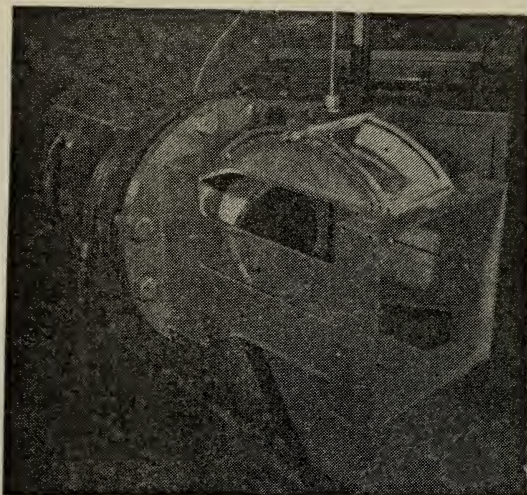


A. Swirl annulus

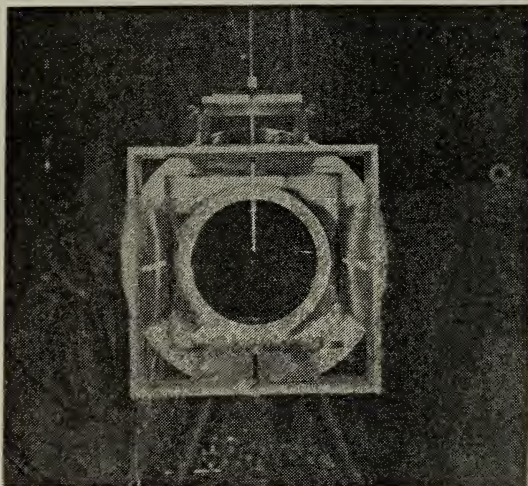


B. End view (a) straight annulus (b) swirl annulus  
FIG. B3. Swirl annulus.





A. Oblique view



B. End view

FIG. B4. Probe mounting box



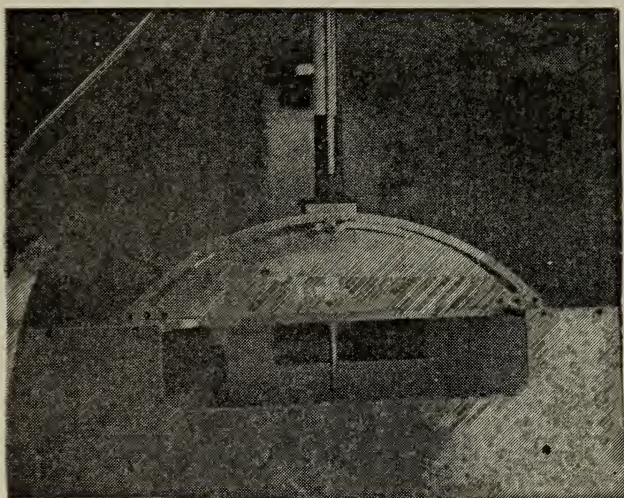


FIG. B5. Pitch angle survey mount.



APPENDIX C  
Computer Programs

The programs outlined below give a simplified, organized method for taking raw data from the combination probe measurements; storing the raw data on the mass memory at the Turbopropulsion Laboratory; reducing the stored data; producing sets of calibration coefficients for the probe; and applying the coefficients to polynomial expressions in general reduction programs. The programs listed were specifically developed for application on the Hewlett-Packard Model 9830A calculator, mass memory, and X-Y plotter.

The raw data from the combination probe measurements was hand recorded and stored in the units of inches of water in the following format.

1.  $\emptyset$  (pitch angle)
2. Pr-Pa
3. Pl-Pa
4. Pl-P23
5. Pl-P4
6. Pa (barometric pressure)
7.  $T_t$  (total temp. (ref.))
8. DT (Delta temp. in microvolts)

Transonic compressor data was automatically recorded on paper tape (Section I). The data and programs used for the



calibration of the probe and data reduction are stored on the mass memory platter entitled "Trans. Comp. Rig., Plat.#3, DodgeØ" at the Turbopropulsion Laboratory data reduction center. A listing of the programs and data files is given and the function of each is explained.

### Computer Programs

- REPROØ - This is the general data reduction program. The calibration coefficients are included in this program as data statements. The program is then utilized to reduce all probe measurements to a set of data that is further reduced by the programs REPRO1 and REPRO2.
- REPRO1,2 - This program obtains reduced data from REPROØ and further reduces it to values that describe the flow conditions at station 2 in the Transonic Compressor.
- REPRO3 - This program reduces data (from a known flow) for the purpose of comparison with "actual" values of  $X$ ,  $\beta$ ,  $\gamma$ , and Mach number. These values are subsequently compared with the derived values of  $X$  and  $\phi$  from the program REPROØ.
- PLOT10 - This program retrieves data from a given data file and transfers the data into the calculator memory in two arrays (POLYGA and POLYGD). These arrays of data can then be conveniently plotted and curve fit using a polynomial regression plotting routine.



- KEY POLY GK - This is a key program which is loaded into the calculator in conjunction with PLOT1Ø. The program retrieves data from the arrays POLYGA and POLYGD in designated numbers of data sets and data points. It plots the data, curve fits the data, and evaluates the coefficients from the fitted curves.
- DODGE7 - This program is a general plotting program which can be modified as desired to plot various sets of derived data in the form of curves and then plot the actual data points against these curves for comparison (see Fig. 28).
- DODGEØ, 1,2,3,4,5,6,8 - These programs consist of various subroutines or reduced sections of the main program REPROØ. They can be utilized individually in the calibration process to check the accuracy of coefficients or make a simple data reduction without having to use the entire general reduction program. Each program is appropriately titled and its purpose is given when it is "listed" from the calculator keyboard.

#### Data Files

- RAWDA1 - Raw data from a probe survey is always initially stored in this file. The "DCOPY" function is then used to transfer this data to the next available RAWXXX file for permanent storage.



The reduction programs REPRO $\emptyset$  and REPRO1 then reduce the data stored in RAWDA1. The file can then be "killed" and reopened for the next set of raw data that requires reduction.

- REDAT1 - Data which is reduced by the programs REPRO $\emptyset$  and REPRO1 is initially stored in this file. The "DCOPY" function is then used to transfer the reduced data to the next available REDAT\_ file for permanent storage.
- BETAX\_ - These files are used to store  $\beta$ ,  $\gamma$ , and  
GAMMP\_ temperature values and coefficients which have  
BETCO\_ been calculated from the key program POLYGK.  
GAMCO\_ The data is entered into these files from the  
TEMCO\_ keyboard with other values from which further  
plots can be made.
- BETGAM - These are additional files on which reduced  
TEMP data from the reduction programs is stored.  
VALUES The data can be retrieved at the users conven-  
PLXD ience or destroyed since it is regenerated  
PLGD each time a particular set of raw data is  
reduced.

The programs and data files listed above form the basis for the calibration and reduction of data obtained by the combination probe. The only changes that may be required when using the programs occur in the dimension statements



which specify the size of an array and in the file statements which specify where particular data is stored.



## BIBLIOGRAPHY

1. Naval Postgraduate School Report NPS-57Sf73072A, Calibration of Flow Nozzles using Traversing Pitot-static Probes, by R. P. Shreeve, July 1973.
2. AIAA Abstract, Calibration and Application of Multiple-Sensor Pneumatic Probes for Velocity Determination with Corrections for Boundary Effects, by R. P. Shreeve and others, January 1976.
3. Naval Postgraduate School Thesis, Velocity Measurements in a Transonic Compressor using a Calibrated Pressure Probe, by D. J. Anderson, March 1976.
4. Naval Postgraduate School Report NPS-57Va72091A, A Description of the Turbopropulsion Laboratory in the Aeronautics Department at the Naval Postgraduate School, by M. H. Vavra and R. P. Shreeve, September 1972.
5. Naval Postgraduate School Thesis, Microprogrammable Data Acquisition and Probe Control System (MIDAS IV) with Application to Compressor Testing, by D. D. Patton, March 1976.
6. Boeing Scientific Research Laboratories Document DL-82-0945, Stagnation Temperature Measurement at High Mach Numbers Using Very Small Probes, by R. P. Shreeve and D. W. Peecher, January 1970.
7. The Boeing Company, Hypersonic Tunnel Projects Log, Fine Wire Thermocouples, by D. W. Peecher, July 1968.



INITIAL DISTRIBUTION LIST

	No. Copies
1. Defense Documentation Center Cameron Station Alexandria, Virginia 22314	2
2. Library, Code 0142 Naval Postgraduate School Monterey, California 93940	2
3. Department Chairman, Code 67 Department Aeronautics Naval Postgraduate School Monterey, California 93940	1
4. Assoc. Professor R. P. Shreeve, Code 67Sf Department of Aeronautics Naval Postgraduate School Monterey, California 93940	1
5. LT F. J. Dodge 12436 Lambuth Road Oakdale, California 95361	1
6. Mr. J. E. Hammer, Code 67 Department of Aeronautics Naval Postgraduate School Monterey, California 93940	1
7. Turbo-Propulsion Laboratory Naval Postgraduate School Monterey, California 93940	10
8. Dr. H. J. Mueller Code 310A, Naval Air Systems Command Navy Department Washington, D.C. 20360	1
9. Mr. Karl H. Guttman Code 330C, Naval Air Systems Command Navy Department Washington, D.C. 20360	1
10. Mr. Eric Lister R & T Division Naval Air Propulsion Test Center Trenton, New Jersey 08628	1



Thesis

D617 Dodge  
c.1

Development of a temperature-pneumatic probe and application at the rotor exit in a transonic compressor.

165676

Thesis

D617 Dodge  
c.1

Development of a temperature-pneumatic probe and application at the rotor exit in a transonic compressor.

165676

thesD617

Development of a temperature-pneumatic p



3 2768 001 89442 1

DUDLEY KNOX LIBRARY